

**Performance Investigation of Flat Plate Solar Collector using vegetable oil-  
based nanofluids**

by

Wan Amirul Asyraf bin Wan Basiron

23083

Dissertation submitted in partial fulfilment of  
the requirements for the  
Bachelor of Mechanical Engineering with Honours

JANUARY 2020

Universiti Teknologi PETRONAS

32610 Seri Iskandar

Perak Darul Ridzuan

**CERTIFICATION OF APPROVAL**

**Performance Investigation of Flat Plate Solar Collector using vegetable oil-  
based nanofluids**

by

Wan Amirul Asyraf bin Wan Basiron

23083

A project dissertation submitted to the  
Mechanical Engineering Programme  
Universiti Teknologi PETRONAS  
in partial fulfilment of the requirement for the  
Bachelor of Mechanical Engineering  
with Honours

Approved by,



---


(Dr. Khairul Habib)

UNIVERSITI TEKNOLOGI PETRONAS  
TRONOH, PERAK

January 2020

**CERTIFICATION OF ORIGINALITY**

This is to certify that I am responsible for the work submitted in this project, that the original work is my own except as specified in the references and acknowledgements, and that the original work contained herein have not been undertaken or done by unspecified sources or persons.

A handwritten signature in black ink, reading "Wan Amirul", written in a cursive style. The signature is positioned above a horizontal line.

WAN AMIRUL ASYRAF BIN WAN BASIRON

## TABLE OF CONTENTS

|   |             |
|---|-------------|
| <b>CERTIFICATION OF APPROVAL .....</b>  | <b>i</b>    |
| <b>CERTIFICATION OF ORIGINALITY .....</b>   | <b>ii</b>   |
| <b>LIST OF FIGURES .....</b>  | <b>iv</b>   |
| <b>LIST OF TABLES .....</b>   | <b>vi</b>   |
| <b>ABSTRACTS .....</b>  | <b>vii</b>  |
| <b>ACKNOWLEDGEMENT .....</b>  | <b>viii</b> |
| <b>CHAPTER 1: INTRODUCTION.....</b>   | <b>1</b>    |
| 1.1 Background.....   | 1           |
| 1.2 Problem Statement.....  | 3           |
| 1.3 Objectives .....  | 3           |
| 1.4 Scope of Study .....  | 3           |
| <b>CHAPTER 2: LITERATURE REVIEW .....</b>   | <b>4</b>    |
| 2.1 Fundamental study and effects of size and volume fraction of the nanoparticles on solar collector ..... | 4           |
| 2.2 Fundamentals of vegetable oil stability and its properties.....   | 7           |
| 2.3 Stability enhancement for oil-based nanofluids .....  | 8           |
| 2.4 Thermophysical study among conventional working fluids.....   | 10          |
| 2.5 Choosing the right vegetable oils .....   | 11          |
| 2.6 Single nanoparticles, oxide nanoparticles and hybrid nanoparticles ...                                  | 13          |
| 2.7 Thermophysical properties of base fluids and nanoparticles.....   | 15          |
| <b>CHAPTER 3: METHODOLOGY .....</b>   | <b>16</b>   |
| 3.1 Research Framework and Process flow .....   | 16          |
| 3.2 Related formula for thermophysical properties estimation for simulation .....                           | 17          |
| 3.3 Thermophysical properties program calculator .....  | 20          |
| 3.4 Thermophysical properties of vegetable oil .....  | 21          |
| 3.5 Assumption and surrounding condition properties.....  | 22          |
| 3.6 Design configuration and schematic diagram.....   | 22          |
| 3.7 Modelling and geometry construction .....   | 23          |
| 3.5 Boundary condition .....  | 25          |
| 3.6 Mesh generation and dependency test .....   | 26          |
| 3.6 Radiation modelling in Ansys Fluent .....   | 29          |
| 3.7 Gantt Chart.....  | 29          |

|  |           |
|--|-----------|
| <b>CHAPTER 4: RESULT AND DISCUSSIONS.....</b>                                      | <b>32</b> |
| 4.1 Convergence graph .....  | 32        |
| 4.2 Contour distribution of water as the working fluid .....                       | 33        |
| 4.3 Code validation .....  | 35        |
| 4.4 Vegetable oil based nanofluids efficiency vs nanoparticles concentration ..... | 36        |
| 4.5 Temperature difference of different nanofluids.....                            | 39        |
| 4.6 Temperature contour distribution of vegetable oils .....                       | 40        |
| 4.7 Efficiency comparison among conventional fluids .....                          | 42        |
| 4.8 Discussions .....  | 43        |
| <b>Chapter 5: CONCLUSION AND RECOMMENDATIONS.....</b>                              | <b>44</b> |
| 4.1 Conclusion .....   | 44        |
| 4.2 Recommendations .....  | 45        |
| <b>REFERENCES.....</b>   | <b>46</b> |
| <b>APPENDICES .....</b>  | <b>49</b> |

## LIST OF FIGURES

|  |    |
|--|----|
| FIGURE 1.1. Flat Plate Solar Collector .....   | 1  |
| FIGURE 2.1. Solar collector efficiency vs volume fraction graph.....   | 5  |
| FIGURE 2.2. Solar collector efficiency vs particle diameter graph .....  | 6  |
| FIGURE 2.3. (A) Electrostatic stabilization<br>(B) Steric stabilization .....  | 8  |
| FIGURE 2.4. (A) Density vs Temperature of various vegetable oil<br>(B) Specific Heat Capacity vs Temperature of various vegetable oil<br>(C) Dynamic viscosity vs Temperature of various vegetable oil<br>(D) Thermal conductivity vs Temperature of various vegetable oil . | 12 |
| FIGURE 3.1. Process flow of the project framework .....  | 16 |
| FIGURE 3.2. Interface of the thermophysical of nanofluids program calculator ....  | 20 |
| FIGURE 3.3. Cell is linked with nanofluids formula .....   | 20 |
| FIGURE 3.4. Schematic diagram of the design configuration .....  | 23 |
| FIGURE 3.5. 3D flat plate solar collector geometry construction .....  | 24 |
| FIGURE 3.6. Mesh generation of the whole solar collector .....   | 26 |

|   |    |
|---|----|
| FIGURE 3.7. Smaller mesh size for the tube .....  | 26 |
| FIGURE 3.8. Mesh dependency test graph .....  | 28 |
| FIGURE 3.9. Solar Calculator in Ansys FLUENT .....  | 29 |
| FIGURE 4.1. The iterations graph from Ansys FLUENT .....  | 32 |
| FIGURE 4.2. The number of iterations to converge .....  | 32 |
| FIGURE 4.3. Temperature contour distribution of the absorber plate .....  | 33 |
| FIGURE 4.4. Temperature contour distribution of the fluid .....   | 34 |
| FIGURE 4.5. Pressure contour distribution of the fluid .....  | 34 |
| FIGURE 4.6. Validation Test Result .....  | 35 |
| FIGURE 4.7. FPSC Efficiency vs Concentration % of Single Nanofluids<br>(Cu-Soybean Oil) .....   | 36 |
| FIGURE 4.8. FPSC Efficiency vs Concentration % of Oxide Nanofluids<br>(CuO-Soybean Oil) .....   | 37 |
| FIGURE 4.9. FPSC Efficiency vs Concentration % of Hybrid Nanofluids<br>(Cu-Zn-Soybean Oil) .....  | 38 |
| FIGURE 4.10. Temperature Difference for different working fluids .....  | 39 |
| FIGURE 4.11. (A) Temperature distribution of single nanofluid at 1.5%<br>concentration (B) Temperature vs length of the solar collector . | 40 |
| FIGURE 4.12. (A) Temperature distribution of oxide nanofluid at 1.5%<br>concentration (B) Temperature vs length of the solar collector .  | 41 |
| FIGURE 4.13. (A) Temperature distribution of hybrid nanofluid at 1.5%<br>concentration (B) Temperature vs length of the solar collector . | 41 |
| FIGURE 4.14. Working fluids efficiency comparison .....   | 42 |
| FIGURE A. 2D Drafting of the flat plate solar collector .....   | 49 |
| FIGURE B. Coordination commands in Ansys Gambit.....  | 49 |
| FIGURE C. Specifying boundary type in Ansys Gambit .....  | 50 |
| FIGURE D. Example of program calculator with values .....   | 50 |
| FIGURE E. Example of result retrieved from Ansys.....   | 50 |
| FIGURE F. File, Mesh and Physic Report from Ansys Fluent.....   | 51 |
| FIGURE G. Mesh transcript from Ansys GAMBIT .....   | 51 |

## LIST OF TABLES

|   |    |
|---|----|
| TABLE 2.1. Table of nanoparticles size .....                        | 6  |
| TABLE 2.2. Comparison table among conventional working fluids ..... | 10 |
| TABLE 2.3. Thermophysical of base fluids and nanoparticles .....    | 15 |
| TABLE 3.1. Thermophysical Properties of Single Nanofluid .....      | 21 |
| TABLE 3.2. Thermophysical Properties of Oxide Nanofluid .....       | 21 |
| TABLE 3.3. Thermophysical Properties of Hybrid Nanofluid.....       | 21 |
| TABLE 3.4. Solar collector components properties .....              | 22 |
| TABLE 3.5. Flat plate solar collector dimension .....               | 25 |
| TABLE 3.6. Mesh dependency test data .....                          | 27 |
| TABLE 3.7. FYP I Gantt chart .....                                  | 30 |
| TABLE 3.8. FYP II Gantt chart .....                                 | 31 |

## **ABSTRACT**

This project will illustrate the practicality of vegetable oil-based (Soybean oil) nanofluid with few nanoparticles including the single-type nanoparticles (Cu), oxide nanoparticles (CuO) and hybrid nanoparticles (Cu-Zn) on the performance of flat plate solar collector as an alternative for conventional working fluid. A numerical study of the vegetable oil-based nanofluid as the working fluid is conducted to visualize the temperature distributions and the efficiency of the flat plate solar collector by using specific formula. The thermophysical properties value of the nanoparticles is obtained from the classical model formula as there are lack of research paper that use vegetable oil as the based nanofluid in the experimental work. Finally, the project concluded that vegetable oil-based nanofluid is feasible as the alternative of the conventional fluid which water that has poor freezing point.



## ACKNOWLEDGEMENT

First, I would like to express my deepest gratitude to Dr. Khairul Habib for guiding me from I had no knowledge about nanofluids. He is indeed a great teacher of its expert field which is heat transfer and always monitor our progress updates to give the best support. Besides, I would like to thank Dr. Aklilu Tesfamichael Baheta, my sporting Energy Conversion lecturer and Final Year Project examiner that keeps on shedding the light and highlight the important points of nanofluid studies especially during proposal defence period. Also, a big thanks to my beloved parents, Wan Basiron bin Wan Ahmad and Wan Noor Paizan binti Wan Sulaiman who understand me well that doing Final Year Project requires a lot of time and focus especially when I am at home. Doing work from home is not as easy as people see because the surrounding is different when we had no friends around that also struggling to finish the last race of the semester. Next, I also feel very thankful to have a supportive friend, Muhammad Syahir bin Saifuddin for keep supporting me when I found it difficult to do the task that is given to me. Not to forget, I would like to thank Dr. Khairul Habib's student, Sabbir for willing to spend a lot of times even during the night when I got trouble with the result achieved from simulation. He portrays a very good personality and always calm in tackling the problems that others had. Lastly, I would like to thank Dr. Tamiru Alemu, the best Final Year Project II coordinator who consistent in delivering new updates and information regarding the Final Year Project even during the Restrict Movement Order, due to Covid-19. I hope that everyone who helped me out and lent me a shoulder will be endowed blessings from Him and protected from any difficult

## CHAPTER 1: INTRODUCTION

### 1.1 Background

Solar thermal energy plays important roles in today's technological world because it is renewable, sustainable and clean. This form of energy utilizes the solar energy to generate thermal energy and produce electric energy for the households, industries and commercial area. The most known solar collector that is widely used is flat-plate solar collector and it can be found almost everywhere especially at the residential area. The main application of flat-plate solar collector is to collect the solar energy and utilize it for heating purpose in the working area with the working temperature range of  $30^{\circ}\text{C}$  to  $100^{\circ}\text{C}$  (Ahmed Kadhim, 2016). For most residential area and small commercial, flat plate solar collector is chosen due to the low cost, installation practicality and simple design compared to other form of water heating system.

Flat-plate solar collector consists of a glass cover plate, flow tubes, absorber plate, insulation plate and the housing. The glass cover is used to transmit vast amounts of short waves light spectrum and provide a greenhouse effect to trap the radiated heat inside the collector. The heat will be absorbed by the absorber plate and transfer it to the working fluid inside the tube. The commonly used working fluid is water because of the good thermophysical physical properties. However, in some cases reported water freezes during winter season hence damaged the tube system of the flat plate collector.

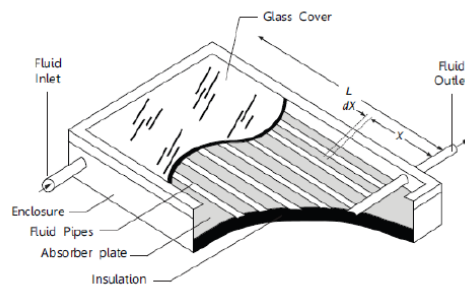


FIGURE 1.1. Flat Plate Solar Collector

Vegetable oil as an alternative is proposed to provide the good performance as the working fluid. It is extracted from different type of seeds or from a part of fruits. There are many types of vegetable oils which are corn oil, grape seed oil, hazelnut oil, linseed oil, rice bran oil safflower oil, sesame oil, canola oil, soybean oil and carapa oil. Vegetables oil had been recognized throughout the days as a potential source of the thermal working fluid due to the good specific heat capacity, biodegradability, environmentally friendly, availability and renewable. Due to the ability to mix with nanoparticles, the thermophysical properties of vegetable oil can be enhanced in this project discussion.

Besides, vegetable oil can be dispersed with various type of nanoparticles for example, Cu, Zn, Al, CuO and many more. According to Choi (1995), “Nanofluids are a relatively new class of fluids which consist of a base fluid with nano-sized particles (1–100 nm) suspended within them. These particles, generally a metal or metal oxide, increase conduction and convection coefficients, allowing for more heat transfer out of the coolant”. Since solid metal such as Cu, Zn, and Al is known with the high thermal conductivity, suspending fine metallic nanoparticles in the working fluid is expected to produce better thermal conductivity enhancement than non-metallic particles.

Nanofluids can be prepared mainly by two techniques to obtain a well dispersion solution. Right preparation method is highly important because as Dhinesh et al. (2016) stated, nanofluids need special necessity and requirements for example stable suspension, less particles agglomeration, an even suspension and no changes in chemical of the working fluid. The first method is one-step method. This method mixes the dispersion of the nanoparticles in the working fluid and the production of the nanoparticles into a single step. Nanofluid that is produced by the solidification of the nanoparticles which is in gaseous phase at the beginning inside their respective base fluid is called direct evaporation one-step method. The original idea was developed by Akoh et al. (1978) when they decided to produce nanoparticles. Meanwhile for the next method, which is two-step method nanoparticles are obtained first and then disperses it into the intended base fluid. Nanoparticles is packed as nano-powders and it can be obtained from different mechanical, physical or chemical sectors.

## **1.2 Problem Statement**

The problem statements of this project are:

- The efficiency of solar collectors is limited by poor freezing point of the conventional working fluid which can damage the piping system during winter
- Lack of theoretical study and research on the effect of vegetable oil as heat transfer medium

## **1.3 Objectives**

The objectives of this project are:

- To study the fundamental and select the best vegetable oil-based nanofluids (Cu, CuO, Cu-Zn)
- To develop simulation model of performance of the vegetables oil-based nanofluids in the flat plat solar collector under different percentage concentration
- To compare and analyse the performance of the flat plate solar collector by using different type of nanoparticles (Cu, CuO, Cu-Zn) in vegetable oil-based fluid

## **1.4 Scope**

- Focus on heat transfer of the working fluid inside the solar collector rather than the whole component
- The modelling and simulation of heat transfer between the system and the heat transfer fluid will be analysed using CFD simulation (ANSYS Fluent)
- Use flat plate solar collector efficiency formula for the performance investigation of the solar collector
- Differentiate the performance of the flat plat solar collector with common based fluid

## CHAPTER 2: LITERATURE REVIEW

### 2.1 Fundamental study and effects of size and volume fraction of the nanoparticles on solar collector

Common working fluids such as water, ethylene glycol, propylene glycol and other heat transfer fluid play one of the most important roles in many diverse industries, including manufacturing, transportation, microelectronics, heating and cooling processes, chemical process, power generation and solid-state lightning. However, these working fluids have restricted thermophysical properties such as low thermal conductivity which result in limited heat exchange rates in today's technology.

As research and development keeps going day by day, researchers had found a way to overcome the limitations by adding ultra-fine solid particles suspended into the common fluids. Saidur et al. (2013) stated that the suspension of the millimeter- or micrometer- sized particles to improve the thermophysical properties of the conventional fluids, has been known for than a decade. The enhanced thermophysical properties of the nanofluids could promote wide range of heat transfer intensification in many areas and one of them is the solar energy devices. Solar collector is a heat exchanger that utilized the solar radiation energy and convert it into internal energy through the working fluid medium. The extracted energy is carried from the working fluid and eventually goes to the hot water equipment or thermal storage, which it usually used during the night or the day with low solar energy. Nanofluids in solar collectors are usually observed in two important aspects which the efficiency and the environmental viewpoints.

The efficiency of the flat plate solar collector is highly depending on the working fluid. Hence, the physical properties result significant effect to the solar collector efficiency. These includes how much and how big nanoparticles are the best suit to be synthesized inside the working fluid.

(a) Volume fraction of nanoparticles

Mahian et al. (2014) plotted and efficiency of mini channel based flat plate solar collector against the concentration of the nanoparticles at 0.1 kg/s mass flowrate. The theoretical study was done by using different type of nanofluids which includes Cu-Water,  $\text{Al}_2\text{O}_3$ -Water,  $\text{TiO}_2$ -Water  $\text{SiO}_2$ -Water. From the result, high solar collector efficiency only achieved at low level of concentration and keep on adding the nanoparticles eventually will cause the efficiency to drop. From the observation also, entropy generations are reduced with the increment of volume concentration. To conclude, too much volume concentration of the nanoparticles in the base fluid may end up deteriorate the thermophysical physical properties as it will significantly increase the value of viscosity. High value of viscosity will cause the difficulty for the fluid to flow hence low viscosity is preferable for a better flow inside the tube and low pump energy consumption.

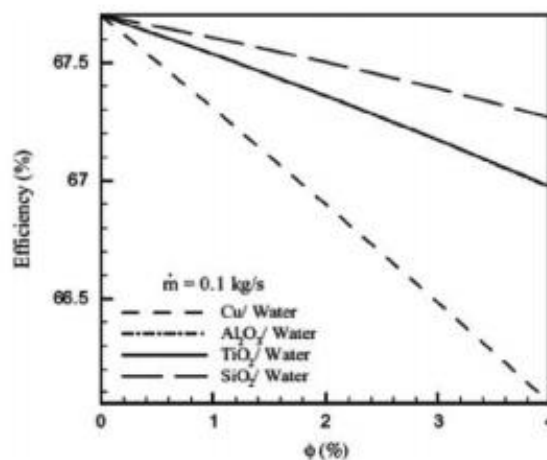


FIGURE 2.1. Solar collector efficiency vs volume fraction graph (Mahian et al., 2014)

(b) Size of nanoparticles

Otanicar et al. (2010) had carried out both experimental and numerical study with different nanofluids to study the performance of a direct absorption solar collector (DASC). The purpose of using different type of nanofluids is to widen the effect of various size of the nanoparticles to the solar collector. The experiments were started with 0.5% volume concentration with smaller particles size. The results of the findings are the smaller size of nanoparticles produced better solar collector efficiency. For better result, adding the volume concentration up to 1% will increase 2 – 4 % of the efficiency. The reduction of the efficiency as the size of the nanoparticles had been explained by the authors which is cause by high fluid absorption at high particle loadings. From the trend, the range of particles size that can maintain a linearity of the efficiency is around 5 to 25 nm.

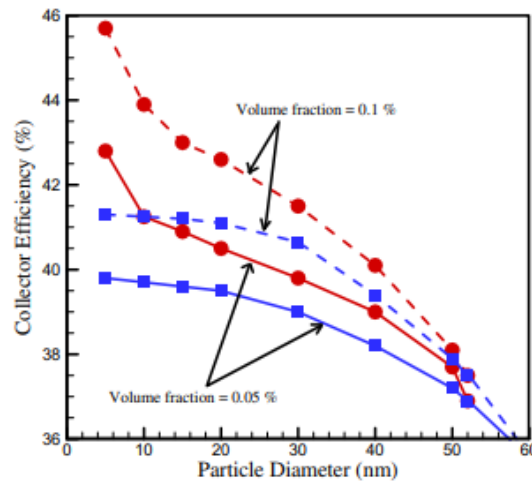


FIGURE 2.2. Solar collector efficiency vs particle diameter graph (Otanicar et al., 2010)

TABLE 2.1. Table of nanoparticles size

| Particle         | Average Particle Size (nm) | Ref                 |
|------------------|----------------------------|---------------------|
| Cu               | 10                         | Choi et al. (2001)  |
| Fe               | 10                         | Hong et al. (2005)  |
| ZnO              | 25                         | Baek et al. (2011)  |
| CuO              | 33                         | Zhang et al. (2006) |
| TiO <sub>2</sub> | 40                         | Zhang et al. (2006) |

## **2.2 Fundamentals of vegetable oil stability and its properties**

Vegetable based natural ester oil has started to be a part of today's research as a working fluid due to the advantages, including biodegradability, higher value in flash point, thermal conductivity, lower calorific value and temperature stability. The availability of vegetable oil is high as it can be produced from renewable sources. Unlike ethylene glycol which is famous with the toxic issue, vegetable oil has the capability to shift and alternate this common working fluid in solar collector as it is environmentally friendly and the thermal conductivity can be enhanced with a way higher when it is dispersed by the right nanoparticles. Sandeep et al. (2016) had done an experiment to study the thermal conductivity enhancement with various oil and the result produced an enhancement of 53% of thermal conductivity and the best increment of flash points with Cu-Zn (50:50) particles.

In terms of the chemical oxidative stability of vegetables oil, it is affected by the change in temperature and the different heating techniques and extraction processes (Bakhshabadi et al., 2018). Vegetable oils consist of variation of esters molecule derived from glycerol and have a high degree of unsaturation. Long fatty acids chain is the special characteristic of vegetables oil and heating the oils at high temperature can change the compositions constituents of triglyceride molecules which indirectly alter the physical properties due to the unsaturation degree and position (Fasina et al., 2008). From a study conducted by Saeeda et al. (2019), the physicochemical parameters of vegetable oils changes are showed by the oxidation rate and in their research, corn oil and concluded to have a faster rate of oxidation compared to soybean oil which make it the stability better compared to the corn oil. There is a way to improve the physical changes of the vegetable oil throughout the temperature which is by adding natural anti-oxidants to vegetable oil (Rafiee et al., 2012). Many researchers concluded that the stability of the vegetable oil will be deteriorates at cooking temperature as vegetable oils are commonly used for cooking. However, for a lower working temperature like flat plate solar collector, the stability of the vegetable oils will not affect that much especially to the chemical properties.



To produce a good stability of vegetable oil based nanofluid, the technique of dispersion of oil based nanofluid is steric stabilization. The dispersion of oil based nanofluid is more convenient and effective as oil phase ligands like fatty acid or amine are responsible to conciliate the growth of nanoparticles and cap the synthesized nanoparticles (Fan Yu et al., 2017). Hence, the capped nanoparticles show uniform dispersion within the vegetable oil.

### 2.3 Stability enhancement for oil-based nanofluids

To achieve the best stability of nanofluids is a bit challenging. Even a lot of method had been proposed, there is no general way to achieve a stable performance for any nanofluids. Controlling and understanding the stability of the nanofluids are very crucial especially for the nanofluids that has broader applications temperature. Without proper stability approach, fouling and settlement at the bottom of the fluids might occur and reduce the enhancement of thermal properties. Stability improvement methods are depending on the based type of the fluid. For example, to improve water based nanofluids, introducing charges onto nanoparticles surface is known as one of the effective methods however, for oil-based nanofluids, the best method is by introducing the surface capping ligands or longer polymer chains. (Yu et al., 2017).

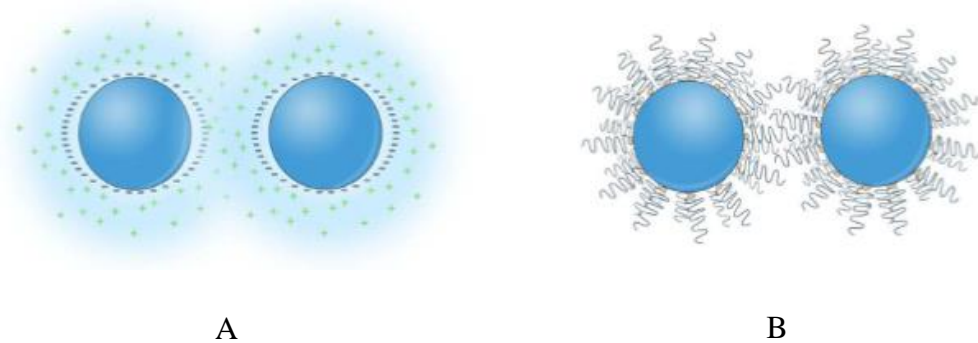


FIGURE 2.3. Schematic of stabilization mechanisms for nanofluids: (A) electrostatic stabilization, (B) steric stabilization (Yu et al., 2017)

Other method had been revealed by a researcher team from Universiti Malaysia Pahang to improve the nanofluid stability is by using ultrasonic vibration process without any surfactant or pH stabilizer. (Sharif et al., 2017). This method is considered as mechanical approach as there is no surface modification required. The stability was observed by using 4-step UV-Vis spectral absorbency analysis and the fluid that was under the observation is PAG lubricants (oil based) with the dispersion of SiO<sub>2</sub> nanoparticles. The ultrasonic vibration process is done for two hours and the result from the approach is the nanofluids are still stable after 30 days without any agglomeration.

In an experiment done by Sandeep et al. (2016), hybrid nanofluid had been prepared by using three different oil-based which are vegetable oil, paraffin oil and SAE oil. All nanofluids are prepared under same concentration which is 0.5%. The method that they used is by using Sodium Dodecyl Sulfate (SDS) surfactant. This is considered as chemical approach which surfactant are added. Surfactant is believed to increase the stability of most nanofluids however, viscosity will be increased too which is not suitable for fluid flowing scenario. In their experiment, vegetable had achieved the highest thermal conductivity among other three nanofluids. However, the stability of all three nanofluids ends until 72h. This experiment shows that using surfactant to improve stability may not work effectively on oil based nanofluids unless the application is needed for less than three days.

Another study that combine both of chemical and mechanical approach had been done by Ghasemi et al. (2015). The based fluid of transformer oil is used along with Fe<sub>3</sub>O<sub>4</sub> nanoparticles under different volume concentrations. The objective of his research is to study the lightning impulse breakdown voltage by using magnetic nanofluids based on transformer oil. They briefed few steps in preparing the nanofluids by coated with oleic acid surfactant and dispersed using an ultrasonic processor. By using both approaches, the stability of the nanofluids was achieved longer than four months. To enhance the stability further, Muthukumaran et al. (2012) claimed that appropriate washing of the as-synthesized to remove the excessive synthetic surfactant can make the nanofluids stable for more than three years under room temperature.

## 2.4 Thermophysical study among conventional working fluids

TABLE 2.2. Comparison table among conventional working fluids

| Base fluid              | Boiling point, °C | Freezing point, °C | Specific heat capacity (kJ/(kg K)) | Thermal conductivity at 40°C (W/mK) | Dynamic Viscosity at 40°C (mPAs) | Toxicity level | Ref.                     |
|-------------------------|-------------------|--------------------|------------------------------------|-------------------------------------|----------------------------------|----------------|--------------------------|
| Vegetable Oil (Soybean) | 240               | - 16               | 2.27                               | 0.162                               | 12                               | None           | Mashewary et al., (2017) |
| Water                   | 100               | 0                  | 4.19                               | 0.625                               | 0.75                             | None           | Yua et al., 2017         |
| Ethylene Glycol         | 197.6             | -12.9              | 2.36                               | 0.250                               | 9.5                              | High           | Ahmadi et al., 2018)     |
| Propylene Glycol        | 182               | -59                | 2.5                                | 0.315                               | 14.28 (with 50% water)           | Low            | Ahmadi et al., 2018)     |

In flat plate solar collector, the common working fluid is water due to relatively high specific heat capacity, incompressible and infinite availability. However as reported by Vanek et al. (2008), the biggest disadvantage of water as the working fluid is it freezes during winter due to high freezing point and eventually damage the piping system of the solar collector. An effort had been made which is draining down the collector at low solar inputs. Unfortunately, pocket water freezing had caused tube damage which make lot of efforts less effective to the freezing system. Due to the freezing point limitations, some designers had started to shift to ethylene glycol and propylene glycol.

Ethylene glycol works best in solar collector as a working fluid as the specific heat capacity and the thermal conductivity is among the good range compared to other fluids except water. However, the disadvantage of ethylene glycol is the toxicity level is very high and due to this it not suitable for domestic hot water system. On the other hand, propylene glycol has a low toxicity level and has a low degradation rate. However, there is a case reported that when the water supply in the tanks somehow stop, the propylene glycol as the working fluid keep receiving heat from the collector without any pauses. This phenomenon develops two problems which the first one,

glycol becomes more acidic at high temperature and the solutions starts to boil and cause overpressure of the fluid. (Vilppu, 2011).

Vegetable oil with the higher boiling or flash point has the capability to withstand with high temperature when there is unwanted scenario happened to the solar collector due to the high boiling point and low freezing point. The toxicity level is considered as none because vegetable oil is a natural ester and does not harm the environment. Even the specific heat capacity and thermal conductivity is low compared to other working fluid, synthesized the vegetable oil with nanoparticles can improve the limitation as a heat transfer fluid. Vegetable oil has a medium range of dynamic viscosity. Even so, vegetable oil can behave as Newtonian fluid and the change in viscosity with the application of shear force is relatively less and this is one of the strong factors is choosing the best working fluid when mobility should be taken into consideration (Sandeep et al., 2016).

## **2.5 Choosing the right vegetable oils**

Edwin et al. (2013) had done extensive study to achieve the value of the thermophysical properties of vegetable oils: cotton, canola, sunflower, corn, and soybean oils. Since the properties of vegetable oil is affected by the temperature, they had repeated the same process with the interval of 10°C for the experiment of density, specific heat capacity, thermal conductivity and dynamic viscosity. Their findings are very useful as each value was concluded in table rather than graph pattern which make it easy for researchers to do numerical study based from the input value. However, to study the behaviour of each vegetable oil, trends and patterns are created in this paper with the temperature range of 30°C to 80°C to suit the working temperature of flat plate solar collector.

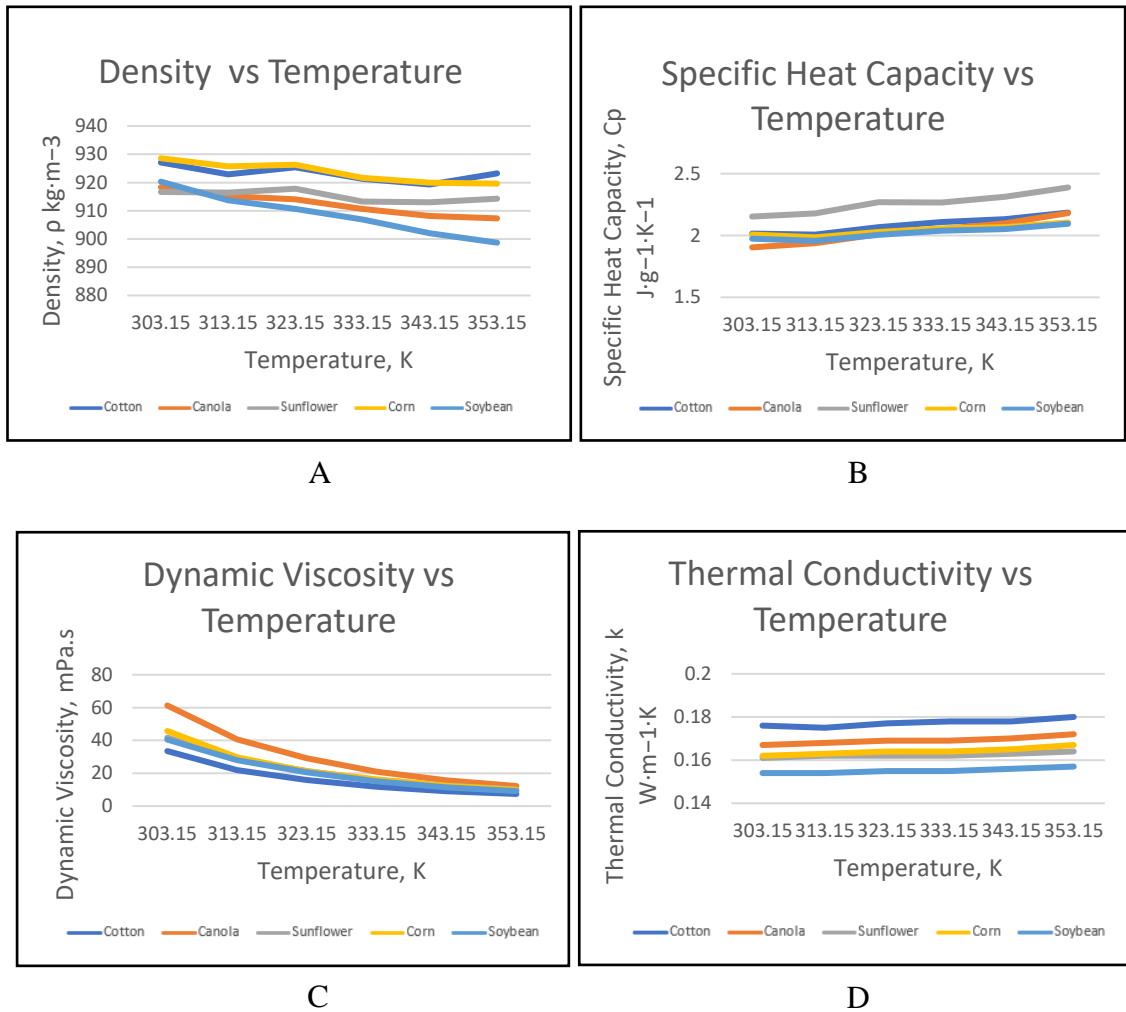


FIGURE 2.4. (A) Density vs Temperature of various vegetable oil  
 (B) Specific Heat Capacity vs Temperature of various vegetable oil  
 (C) Dynamic viscosity vs Temperature of various vegetable oil  
 (D) Thermal conductivity vs Temperature of various vegetable oil  
 (Edwin et al., 2013)

From these trends, all vegetable oils do not differ to much in terms of thermophysical properties. However, when it comes to choose the right application for the vegetable oil, small discrepancy should be considered. In this project, soybean oil is selected even it has the lowest thermal conductivity among the other vegetable oil. Thermal conductivity is not the only scale of measure in heat transfer system of solar collector. The reasons why soybean oil is chosen are, it has a low dynamic viscosity and density. Even canola oil has a good thermal conductivity, the dynamic viscosity produced the highest and similar things goes to cotton oil which has among the highest

density value. The specific heat capacity on the other hand is almost similar for all vegetable oils and all of them increase uniformly throughout the temperature increment. According to Mukesh et al. (2017), soybean oil has a low coefficient of friction and a viscosity of 20% of palm oil which make the mobility better as the working fluid.

## **2.6 Single nanoparticles, oxide nanoparticles and hybrid nanoparticles**

Enhancement of thermal conductivity, specific heat capacity and viscosity are the interesting characteristic of the based fluid synthesized by nanoparticles. The type of nanoparticles affects the percentage enhancement of the thermophysical properties. The common type of synthesized nanoparticles that researchers used to carry out the experiments are single, oxide and hybrid nanoparticles.

### Non-oxide single nanoparticles

Non oxide single nanoparticles synthesizing is a method of adding nanoparticles such as Zn, Cu, Al, Ag and graphite with any oxide components. However, non-oxide nanoparticles dispersed to the base fluid result the lowest enhancement compared to the oxide and hybrid nanoparticles. Kole et al. (2013), had dispersed of Cu nanoparticles alone with the volume concentration of 0.11% to 2% in gear oil and the nanofluid was prepared with surfactant of oleic acid. They found that the thermal conductivity is highly dependent with the temperature as the experiment was carried out at a range of 10°C to 80°C and the enhancement of the thermal conductivity was approximately 24% with 2% of volume concentration at room temperature. According to Taylor et al. (2011), to determine the usefulness of the nanofluids when they are being used in solar collector, the ability to convert solar energy to thermal energy must be known and in their experiments, the measurement of the extinction coefficient for Al, Ag, Au and Cu nanoparticles somehow achieve a good result with the average concentration of 1.0% of volume fraction.

### Oxide nanoparticles

Metal-oxide nanoparticle are widely used in nanofluid field. Thermal conductivity of CuO with engine oil had been studied by Aberoumand et al. (2017) experimentally to observe the effect of the temperature and concentration on the thermal conductivity of the nanofluid. Results achieved from the experiment showed a 49% increase in thermal conductivity with 1% volume concentration in the base fluid. Besides, Kole et al. (2013) examined the conductivity enhancement of CuO on gear oil and the result obtained was 10.4% increment at only 0.025% of volume fraction. This conclude that oxide nanoparticles have a better thermal conductivity increment even it is at a lower volume fraction value. Mu et al. (2009) had carried radioactive properties of oxide nanoparticles which is SiO<sub>2</sub> and compare it with ZrC. SiO<sub>2</sub> allowed a remarkable amount of visible light to pass through the nanofluid compared to ZrC.

### Hybrid nanoparticles

Hybrid nanofluids showed high thermo properties enhancement in comparison with conventional nanofluid. According to Sandeep et al. (2016), hybrid nanofluids of Cu-Zn can be prepared by adding the estimated amount of nano-powders in vegetable oil through ultrasonication method which requires the functionality of ultrasonic probe sonicator for 2 h each. Among paraffin, SAE and vegetable oil, the improvement of flash point vegetables point is the highest with Cu-Zn nanoparticles which made the vegetable oil among the best pair of hybrid nanoparticles. Hybrid nanoparticles of Cu-Zn had improved the relative thermal conductivity to relative viscosity for effective heat transfer especially in vegetable oil as the experimental result of Sandeep et al. (2016) had showed 53% better results in comparison with paraffin and SAE oil with a low concentration value. High concentration value should be avoided as Saedinia et al. (2012) reported that increasing the solid concentration of nanoparticles will decrease the specific heat capacity of the nanofluids.

## 2.7 Thermophysical properties of base fluids and nanoparticles

Calculating the vegetable oil based nanofluids will require the thermophysical properties of the base fluid and nanoparticles. Since in this project requires three different nanoparticles which are Cu, CuO and Zn, those value should be identified so that the properties of single, oxide and hybrid nanofluids can be formulated. Some of the value are retrieved from researchers meanwhile some of it makes us of the functionality material database that are provided from Ansys software. Following is the thermophysical properties of the base fluid and nanoparticles:

TABLE 2.3. Thermophysical of base fluids and nanoparticles

| <b>Properties</b>       | <b>Density (kg/m<sup>3</sup>)</b> | <b>Viscosity (kg/ms)</b> | <b>Thermal conductivity (W/mK)</b> | <b>Specific heat capacity J/kgK</b> | <b>Ref.</b>            |
|-------------------------|-----------------------------------|--------------------------|------------------------------------|-------------------------------------|------------------------|
| Water                   | 998.2                             | 0.001003                 | 0.6                                | 4182                                | Ansys Database         |
| Soybean Oil             | 913.7                             | 0.028001                 | 0.154                              | 1957                                | Edwin et al. (2013)    |
| Copper (Cu)             | 8978                              | N/A                      | 387.6                              | 381                                 | Ansys Database         |
| Copper (II) Oxide (CuO) | 6510                              | N/A                      | 18                                 | 540                                 | Ramasamy et al. (2018) |
| Zinc                    | 7100                              | N/A                      | 112.2                              | 390                                 | Ansys Database         |



## CHAPTER 3: METHODOLOGY

### 3.1 Research Framework and Process flow

Following are the process flow chart of the project progress start from the literature review study until the result from simulation is attained. The modelling and simulation will be done by using Finite Element Modelling and Simulation with ANSYS software.

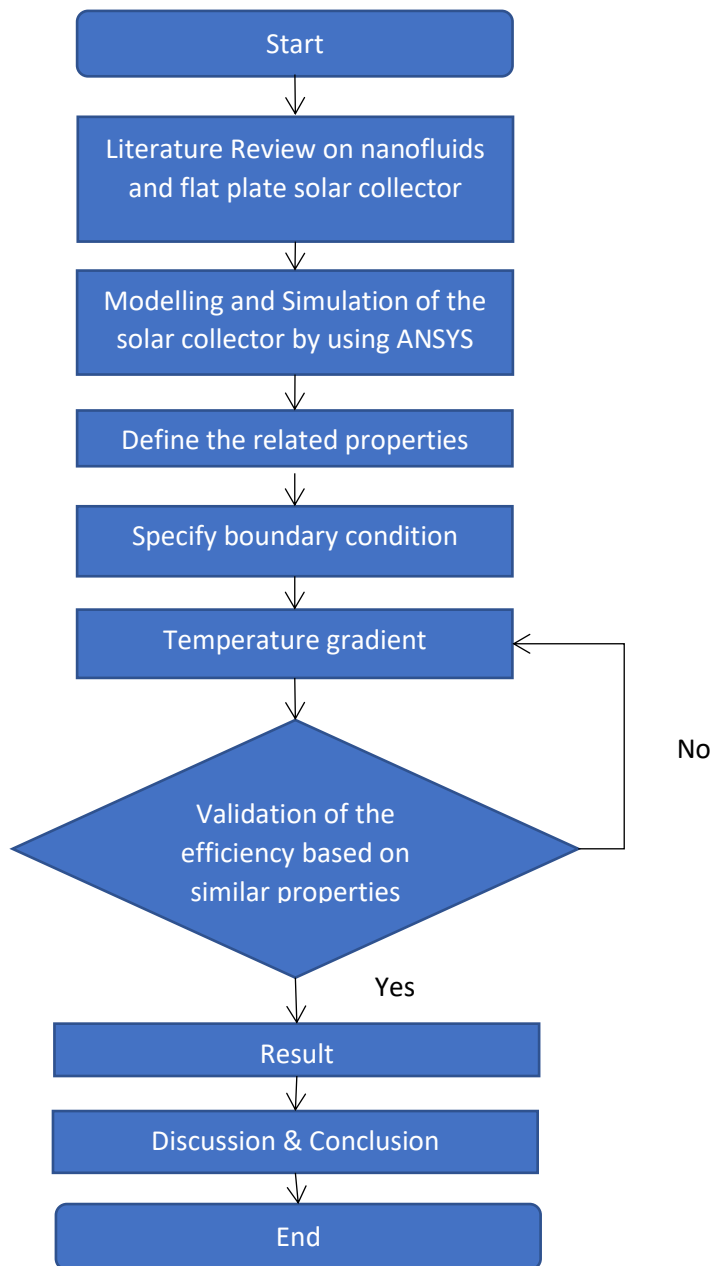


FIGURE 3.1. Process flow of the project framework

### 3.2 Related formula for thermophysical properties estimation for simulation

In this project, the efficiency of the solar collector should be investigated by using vegetable oil-based nanofluid. Soybean is chosen due to the good mobility properties with an acceptable range of thermal conductivity and specific heat capacity. Various type of nanoparticles will be used as synthesized nanoparticle in the soybean oil which including the single non-oxide nanoparticles (Cu), metal oxide nanoparticles (CuO) and hybrid nanofluids of Cu-Zn. However, the limitation is lack of research and study of these combinations which make it difficult to observe the thermophysical properties. Due to extensive research and study, few formulas to predict and estimate are obtained from many researchers to assist this project. Maxwell (1881) had developed formula to obtain the thermal conductivity, density and specific heat capacity of the nanofluids which is observed and had been modified by many researchers throughout for example Hamilton-Crosser (1962) and Takabi and Salehi (2014) as follow:

*Thermal conductivity of conventional nanofluids:*

$$\frac{k_{nf}}{k_{bf}} = \frac{k_p + 2k_{bf} - 2\phi_p(k_{bf} - k_p)}{k_p + 2k_{bf} - \phi_p(k_{bf} - k_p)} \quad (1)$$

*Thermal conductivity of hybrid nanofluids:*

$$k_{hnf} = k_{bf} \left[ \frac{\frac{k_{p1}\phi_{p1} + k_{p2}\phi_{p2}}{\phi_{hnf}} + 2k_{bf} + 2(k_{p1}\phi_{p1} + k_{p2}\phi_{p2}) - 2\phi k_{bf}}{\frac{k_{p1}\phi_{p1} + k_{p2}\phi_{p2}}{\phi_{hnf}} + 2k_{bf} - 2(k_{p1}\phi_{p1} + k_{p2}\phi_{p2}) - \phi k_{bf}} \right] \quad (2)$$

*Density of conventional nanofluids:*

$$\rho_{nf} = \phi_p \rho_p + (1 - \phi_p) \rho_{bf} \quad (3)$$

*Density of hybrid nanofluids:*

$$\begin{aligned}\rho_{hnf} &= \phi_{p1}\rho_{p1} + \phi_{p2}\rho_{p2} + (1 - \phi_h)\rho_{bf} \\ \phi_h &= \phi_{p1} + \phi_{p2}\end{aligned}\quad (4)$$

For the specific heat capacity of nanofluids, the formula had been developed by Pak and Cho (1998) and Takabi and Salehi (2014) as below:

*Specific heat capacity of conventional nanofluids:*

$$c_{p_{nf}} = c_{p_{nf}}\phi + (1 - \phi)c_{p_{bf}} \quad (5)$$

*Specific heat capacity of hybrid nanofluids:*

$$c_{p_{nf}} = \frac{(1 - \phi)\rho_{bf}c_{p_{nf}} + \phi\rho_{p1}c_{p_{p1}} + \phi\rho_{p2}c_{p_{p2}}}{\rho_{hnf}} \quad (6)$$

For the dynamic viscosity of the single nanofluid, the model is following Einstein's model which is popular in predicting spherical nanoparticles. For the hybrid nanofluids, Tekir et al. (2017) proposed a new correlation in their analysis and they use three different approach which are Single Phase Model, Euler-Euler Approach, Euler-Lagrange Approach. Both formulas are given as follow:

$$\mu_{nf} = \frac{\mu_{bf}}{(1 - \phi)^{2.5}} \quad (7)$$

$$\mu_{hnf} = \frac{\mu_{bf}}{(1 - (\phi_{p1} + \phi_{p2}))^{2.5}} \quad (8)$$

To study the performance of the solar collector, the efficiency of flat plate solar collector formula will be used. The inlet temperature value will be taken from other researcher that had been carrying out the experiment of flat plate solar collector by using water as the working fluid. Following is the efficiency of the flat plate solar collector formula:

$$Q_u = \dot{m}c_p(T_{out} - T_{in}) \quad (9)$$

$$\eta = \frac{Q_u}{I_{t,a}A_a} \quad (10)$$

$$\eta = \frac{\dot{m}c_p(T_{out} - T_{in})}{I_{t,a}A_a} \quad (11)$$

### Nomenclature

|             |  |           |                                      |
|-------------|--|-----------|--------------------------------------|
| $k$         | Thermal conductivity ( $\frac{W}{mK}$ )    | $\dot{m}$ | Mass flow rate ( $\frac{kg}{s}$ )    |
| $\rho$      | Density ( $\frac{kg}{m^3}$ )               | $I_{t,a}$ | Solar irradiance ( $\frac{W}{m^2}$ ) |
| $c_p$       | Specific heat capacity ( $\frac{J}{kgK}$ ) | $T_{in}$  | Inlet Temperature (K)                |
| $\mu$       | Dynamic viscosity ( $\frac{kg}{ms}$ )      | $T_{out}$ | Outlet Temperature (K)               |
| $\phi$      | Solid concentration (%)                    | $A_a$     | Area of the collector ( $m^2$ )      |
| $\dot{Q}_u$ | Useful energy collected ( $W$ )            | $\eta$    | Efficiency                           |

### 3.3 Thermal physical program calculator

In this project, vegetable oil based with different type of nanofluids will be simulated under different concentration. Conventional calculation may take some time as the formula is quite long and it is not practical to repeat the same calculation for different concentration. Therefore, a program to calculate the thermophysical properties of the nanofluids is introduced. The governing equation is taken from many previous researchers such as Hamilton-Crosser, Einstein and Takabi and Salehi (2014) from the methodology section. Following is the program interface:

FIGURE 3.2. Interface of the thermophysical of nanofluids program calculator

Following is the example of the formula from one of the cells that has an automatic generate data from user input:

FIGURE 3.3. Cell is linked with nanofluids formula

### 3.4 Thermal properties of nanofluids

By using the governing equation stated in previous chapter, thermal properties data are calculated for the *cell zone condition* and *material properties* in Ansys Fluent. The changes of the properties will affect the result and the behavior of the working fluids. Thermal properties of the different type of nanofluids (Cu-Soybean Oil, CuO-Soybean Oil and Cu-Zn-Soybean Oil) are identified based on different number of concentrations as below:

TABLE 3.1. Thermal Properties of Single Nanofluid

| <b>Single Nanofluids (Cu)</b> |   |                                 |                              |                               |
|-------------------------------|---|---------------------------------|------------------------------|-------------------------------|
| <b>%</b>                      | <b><math>\rho</math> (kg/m<sup>3</sup>)</b> | <b><math>C_p</math> (J/kgK)</b> | <b><math>k</math> (W/mK)</b> | <b><math>u</math> (kg/ms)</b> |
| 0.1                           | 1720.13                                     | 1799.4                          | 0.205265411                  | 0.036439069                   |
| 0.2                           | 2526.56                                     | 1641.8                          | 0.2693281                    | 0.048915734                   |
| 0.3                           | 3332.99                                     | 1484.2                          | 0.351663288                  | 0.068301217                   |

TABLE 3.2. Thermal Properties of Oxide Nanofluid

| <b>Oxide Nanofluids (CuO)</b> |   |                                 |                              |                               |
|-------------------------------|---|---------------------------------|------------------------------|-------------------------------|
| <b>%</b>                      | <b><math>\rho</math> (kg/m<sup>3</sup>)</b> | <b><math>C_p</math> (J/kgK)</b> | <b><math>k</math> (W/mK)</b> | <b><math>u</math> (kg/ms)</b> |
| 0.1                           | 1473.33                                     | 1815.3                          | 0.203898                     | 0.036439                      |
| 0.2                           | 2032.96                                     | 1673.6                          | 0.26588                      | 0.048916                      |
| 0.3                           | 2592.59                                     | 1531.9                          | 0.344939                     | 0.068301                      |

TABLE 3.3. Thermal Properties of Hybrid Nanofluid

| <b>Hybrid Nanofluids (Cu-Zn)</b> |   |                                 |                              |                               |
|----------------------------------|---|---------------------------------|------------------------------|-------------------------------|
| <b>%</b>                         | <b><math>\rho</math> (kg/m<sup>3</sup>)</b> | <b><math>C_p</math> (J/kgK)</b> | <b><math>k</math> (W/mK)</b> | <b><math>u</math> (kg/ms)</b> |
| 0.1                              | 1626.23                                     | 1370.200777                     | 0.230876                     | 0.036439                      |
| 0.2                              | 2338.76                                     | 1140.951752                     | 0.358923                     | 0.048916                      |
| 0.3                              | 3051.29                                     | 1018.770104                     | 0.614722                     | 0.068301                      |

### 3.5 Assumption and surrounding condition properties

To simulate the real condition of the working fluid inside the solar collector, the surrounding condition properties should be known to produce accurate result to the experimental value. The inlet velocity will be used is 0.02 m/s and the physical properties value of related component of solar collector which are absorber plate and glass are studied as follow:

TABLE 3.4. Solar collector components properties

| Properties                    | Absorber Plate<br>(copper) | Glass<br>Plate | Air    | Rockwool |
|-------------------------------|----------------------------|----------------|--------|----------|
| Density, (kg/m <sup>3</sup> ) | 8978                       | 2230           | 1.225  | 48       |
| C <sub>p</sub> (j/kg K)       | 381                        | 750            | 1006.4 | 840      |
| K (W/mK)                      | 387.6                      | 1.14           | 0.0242 | 0.04     |

*Assumption: The flow is assumed steady and the fluid possesses uniform axial velocity  $V_0$  and temperature  $T_0$  profiles at the inlet of tube*

### 3.6 Design configurations and schematic diagram

The configuration of this solar collector is an active configuration as it involves pump. The nanofluid is initially stored in the tank and it flows to the flow control valve and flow meter by pump before entering the flat plate collector. The main function of a flow control valve is to control the flow rate in the flow circuit meanwhile the flow meter acts as an indicator to measure the volume of the nanofluids passing through the line. When the nanofluid enters the collector, it will be heated and enters the secondary tank. The secondary tank serves as and heat exchanger to heat up the cool water comes into the tank and due to the heat transfer phenomenon, hot water will be produced and flows out of the tank.

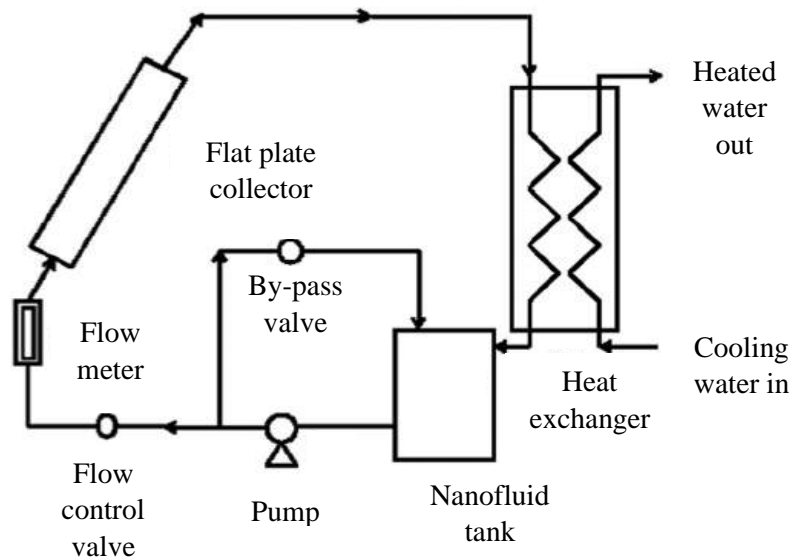


FIGURE 3.4. Schematic diagram of the design configuration

### 3.7 Modelling and Geometry Construction

To simulate the behaviour of the fluid inside the flat plate solar collector, geometry or the model is required. Hence, the geometry of the flat plate solar collector was created by using Ansys GAMBIT software. Ansys GAMBIT is a geometry and mesh generation software that can work together with Ansys FLUENT. There are 5 main components in Ansys FLUENT which are geometry, mesh, setup, solution and results. The ability of the Ansys GAMBIT is it can complete two of the main components required in Ansys Fluent which are geometry and meshing. Unlike, Autocad and Catia, there are only focusing on the geometry construction without having the function to do meshing. A complete set of automated and size function driven meshing software promises an excellent meshing work to be generated whether it is hybrid, structured, unstructured and multiblock.



The geometry construction is initialized with the point plotting according to the dimension of the flat plate solar collector. In real construction, there will be a lot of riser tubes to create the path for the fluid to flow in the solar collector. However, the design can be simplified for only one riser tube for the simulation works without abandoning the cell zone condition like absorber, glass and insulation. This is because, the fluid flow behaviour is similar in other tubes hence simplify the construction may reduce a lot of time. In a research paper by Ekramian et al. (2014), one tube configuration is used for numerical analysis of heat transfer in flat plate solar collectors.

The assumptions for this simplified CFD geometry are:

- 1) Fluid is divided equally through all risers and the flowrate in each riser is constant
- 2) Radiation loss is ignored specifically from margins of collector
- 3) Heat loss is neglected at the bottom surface of collector

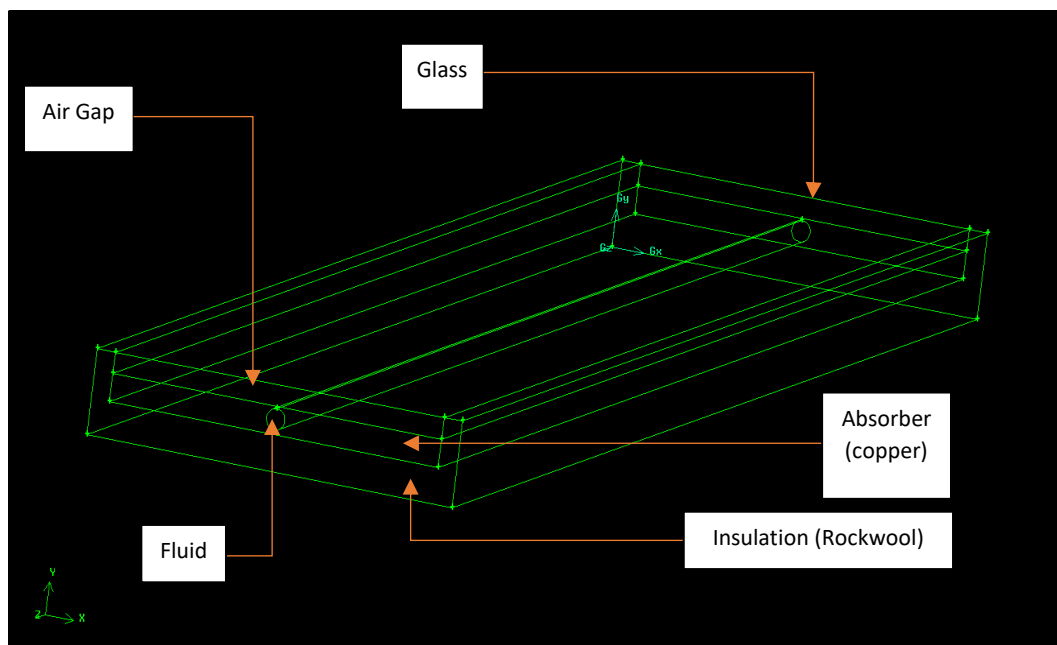


FIGURE 3.5. 3D flat plate solar collector geometry construction

The point plotting is important to create lines and surfaces. The starting point is at the centre of the axis reference with the coordinate of 0, 0 in X and Y axis. To create other points, coordinates of each point is important to create a perfect dimension. The point plotting is created on only two axis which means there are on a single plane of X and Y axis. The lines are connected from point to point to produce faces. From faces, 3D model can be created by using extruding process. Volume is generated from each surface and different volume is assigned with different cell zone for the material specification.

Following are the dimension of the flat plate solar collector:

TABLE 3.5. Flat plate solar collector dimension

| <b>Solar collector design</b> |               |
|-------------------------------|---------------|
| Specification                 | Dimension, mm |
| Width                         | 200           |
| Height                        | 40            |
| Length                        | 1000          |
| Wall Thinkness                | 10            |
| Tube diameter                 | 10            |

### **3.8 Boundary Condition**

When the 3D model has been created with a length of 1000 mm, cell zone can be specified with glass, absorber, tube and insulation from the entity. Starting from the top surface, the material is specified as glass. For the first volume from top is the air and followed by the absorber meanwhile for the bottom and frame volume is specified as insulation which made of rockwool. Next, boundary condition should be specified. In this project, the inlet is chosen to be the “velocity\_inlet” type so that the value of the velocity can be inserted in the simulation. Meanwhile, the outlet was set to default which is “pressure\_outlet” and it will be automatically calculated during simulation. The other components are declared as wall. “Interface\_1” is the wall of the tube meanwhile “Interface\_2” is the wall for the air trap.

### 3.9 Mesh generation

The meshing process was done in Ansys GAMBIT as well. The technique that was used for the meshing is the volume or body meshing. There are four main volumes in the geometry and each of them is meshed according to their priority in the simulation. For example, the tube act as the pathway for the working fluids and the goal of the simulation is to study the outlet temperature of the fluid running inside the tube so that efficiency can be computed. Hence, the mesh of the tube should be created with more detail and smaller size compared to other components in the solar collector. The type of mesh for the tube is “tet/hybrid” or commonly known as tetrahedral/hybrid meshing. The spacing size is selected as interval size function with a value of 0.001 for the tube and 0.003 for the other components.

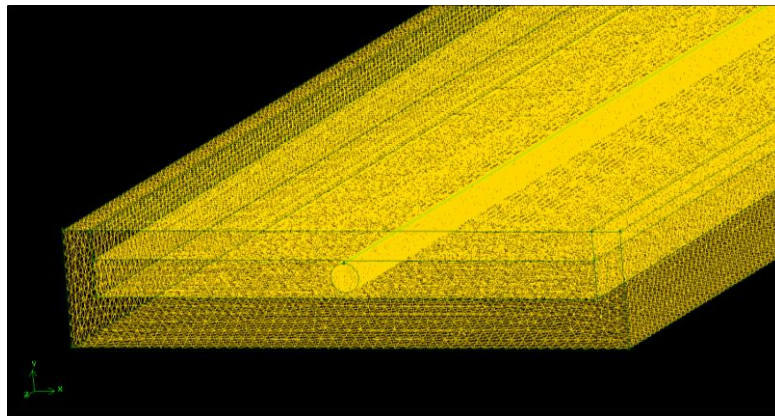


FIGURE 3.6. Mesh generation of the whole solar collector

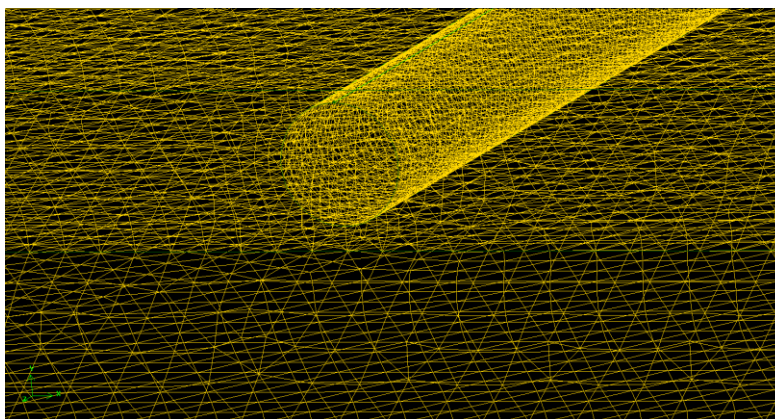


FIGURE 3.7. Smaller mesh size for the tube

Mesh dependency test is a convergence test that is required to determine the least number of elements in finite element modelling that can produce nearly accurate result. There are many factors that affect number of elements for example, element size, number of divisions, number of spacing, type of the mesh finishing (course, medium, fine) and many more. For instance, when we increase the number of divisions in an edge, it will produce high number of elements around it. Hence, the variable of this test is depending on how the mesh is generated or the technique used.

In this test, the variable of the number of elements is the spacing value and some of the settings set as default to reduce the time taken. As mentioned, the mesh is generated by using volume meshing and each of the volume is assigned with different number of spacing according to the role in simulation. Small spacing will result in higher number of elements. Following is the data collected from few tests in the simulation:

TABLE 3.6. Mesh dependency test data

| <b>Tet/<br/>Hybrid</b>                    | <b>Tet/<br/>Hybrid</b>                                  | <b>Hex/<br/>Wedge</b>                    | <b>Tet/<br/>Hybrid</b>                     | <b>Results</b>                    |                                      |                    |
|---|---|--|--|-----------------------------------|--------------------------------------|--------------------|
| <b>Pipe<br/>volume<br/>spacing,<br/>m</b> | <b>Absorber<br/>plate<br/>volume<br/>spacing,<br/>m</b> | <b>Air<br/>volume<br/>spacing,<br/>m</b> | <b>Frame<br/>volume<br/>spacing,<br/>m</b> | <b>Number<br/>of<br/>elements</b> | <b>Outlet<br/>Temperature,<br/>K</b> | <b>Status</b>      |
| 0.002                                     | 0.004   | 0.004                                    | 0.005                                      | 698391                            | 305.08437                            | Converge           |
| 0.003                                     | 0.003   | 0.003                                    | 0.004                                      | 1260062                           | 305.34108                            | Non-<br>converging |
| 0.002                                     | 0.003   | 0.003                                    | 0.004                                      | 1348205                           | 305.13048                            | Converge           |
| 0.001                                     | 0.004   | 0.004                                    | 0.005                                      | 1453828                           | 305.14542                            | Converge           |
| 0.001                                     | 0.003   | 0.003                                    | 0.004                                      | 2118710                           | 305.0014                             | Converge           |
| 0.0008                                    | 0.003   | 0.003                                    | 0.004                                      | 2844964                           | 304.99643                            | Converge           |
| 0.0006                                    | 0.003   | 0.003                                    | 0.004                                      | 4887787                           | 305.00639                            | Converge           |
| 0.001                                     | 0.002   | 0.002                                    | 0.003                                      | 4931698                           | 304.95546                            | Converge           |
| 0.0006                                    | 0.002   | 0.002                                    | 0.003                                      | 7758995                           | 304.94532                            | Converge           |

From the table, it is noticeable that large number of spacing can cause a non-converging result in the simulation. For example, 0.003 m spacing for volume 1 caused a non-converging scenario which is undesirable in any simulation result. Hence, the maximum number of spacing for volume 1 can be concluded as 0.002 m. The higher the number of elements, the longer time taken for the solution to converge. For the same number of spacing 0.001 m for volume 1, few tests are done by reducing 0.001 m for volume 2, 3 and 4.

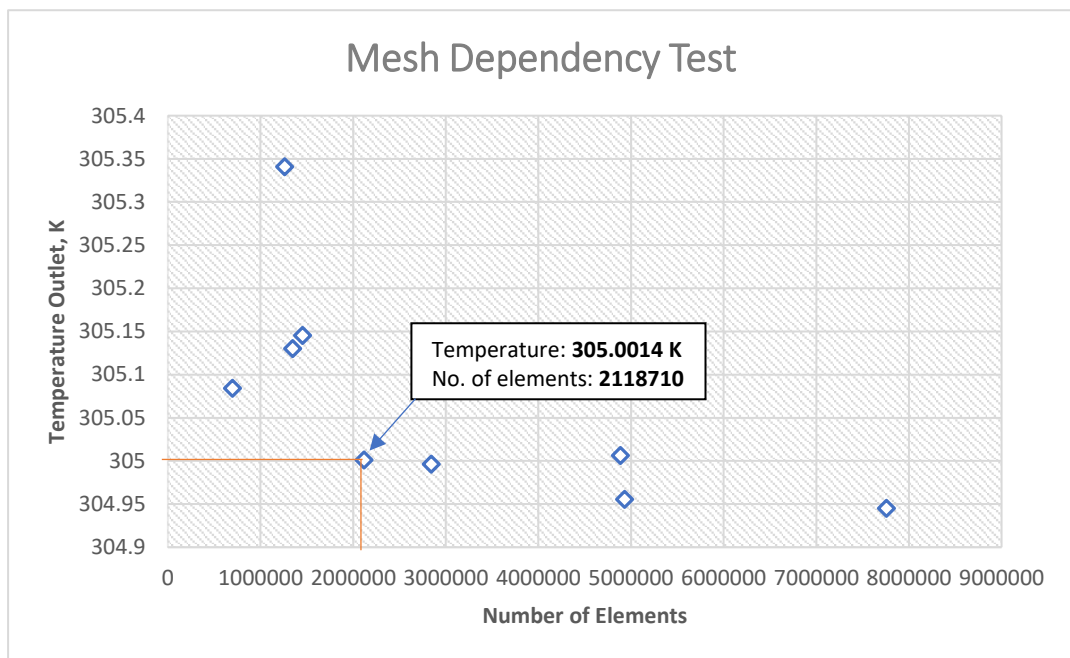


FIGURE 3.8. Mesh dependency test graph

From the trend, the graph starts to stable at around 305 K. Hence, the most preferable element size is 2118710 because the difference with the same number of spacing of 0.001 m for volume 1 with element size of 4931698 is only 0.0459 K and with the number of elements of 7758995 is 0.0561 K which is very small and not worth for a very long duration of convergence. Plus, the chosen element size has the shortest duration of convergence that produce a result of 305 K outlet temperature.

### 3.10 Radiation modelling in Ansys FLUENT

Mesh was imported to Ansys FLUENT to generate the result of the temperature inlet. Material specification details were inserted under Setup Tab in Ansys FLUENT. Under “Models”, energy equation must be turned on as the simulation will deal with the heat transfer and the viscous is set to “k-epsilon” with a default setting instead of laminar to obtain a better accuracy of the result. Radiation model is required to mimic the sun irradiation sent onto the surface of the solar collector. As the result should be validated with another researcher, the location of the experimental work should be known as Ansys FLUENT will automatically generate the direct solar irradiation and diffuse solar irradiation according to the location. However, to study the behaviour of the working fluid inside the collector if they match the characteristic of the solar collector working fluid during simulation, the setting for the radiation is set to 1200 (W/m<sup>2</sup>) for the direct solar irradiation and 200 W/m<sup>2</sup> for the diffuse solar irradiation.

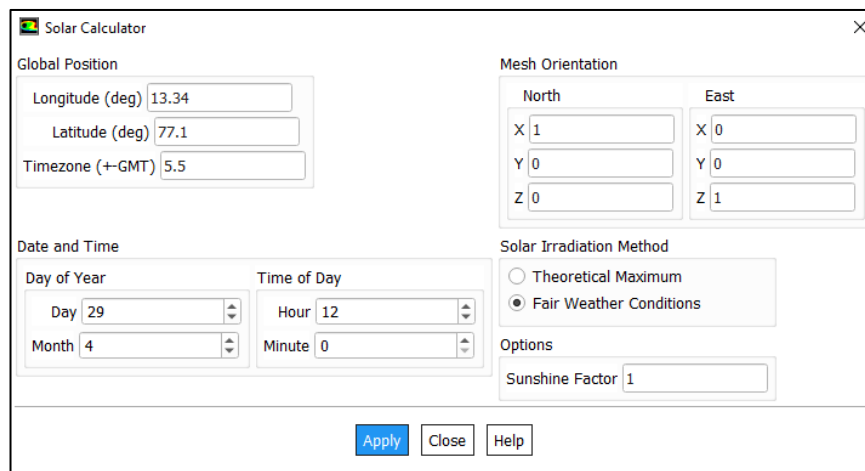


FIGURE 3.9. Solar Calculator in Ansys FLUENT

The value however will be changed accordingly to validate and match the result with other researcher as a code validation under result section. By turning on the radiation model, the trend of the outlet temperature is expected to give similar pattern with experimental data.

### 3.11 Gantt chart

*FYP I*

**Key milestone:** Understand the behaviour of the vegetable oil based with different type of nanoparticles

TABLE 3.7. FYP I Gantt chart

| <i>Activity</i>  | <i>W1</i> | <i>W2</i> | <i>W3</i> | <i>W4</i> | <i>W5</i> | <i>W6</i> | <i>W7</i> | <i>W8</i> | <i>W9</i> | <i>W10</i> | <i>W11</i> | <i>W12</i> |
|--|-----------|-----------|-----------|-----------|-----------|-----------|-----------|-----------|-----------|------------|------------|------------|
| <i>Basic study of nanofluid</i>  | *         |           |           |           |           |           |           |           |           |            |            |            |
| <i>Study on the literature review</i>                                  |           |           | *         | *         |           |           |           |           |           |            |            |            |
| <i>Finalise the nanoparticles</i>                                      |           |           |           |           |           | *         |           |           |           |            |            |            |
| <i>Construct methodology on vegetable oil performance</i>              |           |           |           |           |           |           | *         | *         |           |            |            |            |
| <i>Analyse the properties improvement of the vegetable nanofluid</i>   |           |           |           |           |           |           |           |           | *         |            |            |            |
| <i>Study the performance improvement equation for ANSYS simulation</i> |           |           |           |           |           |           |           |           |           |            | *          | *          |

*FYP II*

**Key milestone:** Model, simulate and analyse the performance investigation of flat plate solar collector with vegetable oil based nanofluid.

TABLE 3.8. FYP II Gantt chart

| <i>Activity</i>  | <b>W1</b> | <b>W2</b> | <b>W3</b> | <b>W4</b> | <b>W5</b> | <b>W6</b> | <b>W7</b> | <b>W8</b> | <b>W9</b> | <b>W10</b> | <b>W11</b> | <b>W12</b> |
|--|-----------|-----------|-----------|-----------|-----------|-----------|-----------|-----------|-----------|------------|------------|------------|
| <i>Finalise ANSYS modelling for the solar collector performance with different type of nanoparticles</i> |           | *         | *         | *         | *         | *         |           |           |           |            |            |            |
| <i>Perform test and result validation</i>  |           |           |           |           |           |           | *         |           |           |            |            |            |
| <i>Analysing the improvement and compare with other nanofluids (Water base)</i>                          |           |           |           |           |           |           |           |           | *         |            |            |            |
| <i>Verification and conclude the performance improvement</i>   |           |           |           |           |           |           |           |           |           | *          |            |            |



## CHAPTER 4: RESULTS AND DISCUSSION

### 4.1 Convergence graph

For the early part of result section, water is used as the working fluid instead of vegetable oil. This is because the model needs to be validated and research paper using vegetable oil in the solar collector is very limited. The setting difference between using water and vegetable oil is only under cell zone boundary section which the fluid can be changed to any fluid that is desired. The result is observed when the iterations reached convergence and usually it takes up to 150 iterations to reach convergence criteria.

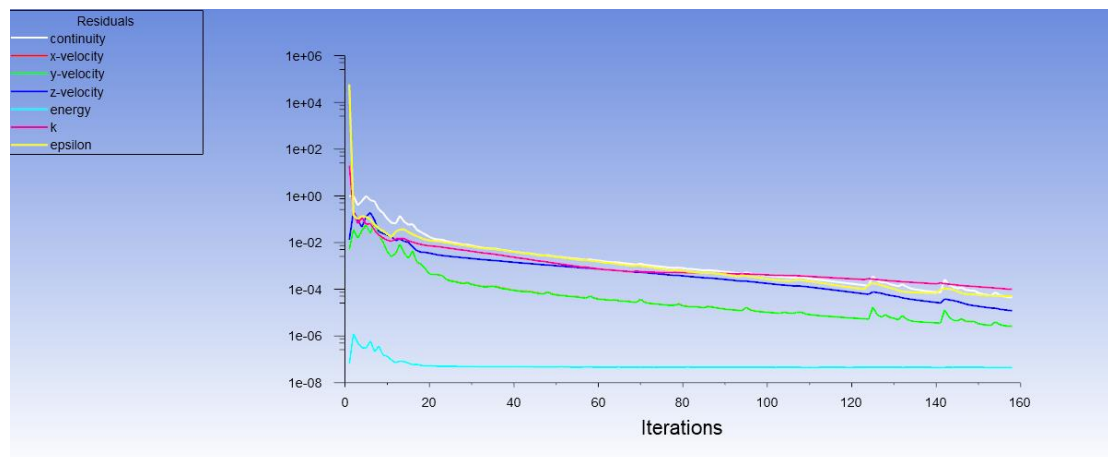


FIGURE 4.1. The iterations graph from Ansys FLUENT

```
iter  continuity  x-velocity  y-velocity  z-velocity  energy  k  epsilon  time/iter
155  5.7190e-05  3.1157e-06  3.1351e-06  1.4125e-05  4.5395e-08  1.0503e-04  5.2615e-05  55:27:22  9845
156  4.9929e-05  2.7679e-06  2.7522e-06  1.3312e-05  4.5566e-08  1.0542e-04  5.1721e-05  55:17:53  9844
157  4.6626e-05  2.6470e-06  2.6770e-06  1.2666e-05  4.5605e-08  1.0189e-04  5.0748e-05  55:43:03  9843
! 158 solution is converged
158  4.4335e-05  2.5805e-06  2.6156e-06  1.2084e-05  4.5514e-08  9.9797e-05  5.0255e-05  55:30:18  9842
Writing data to C:\Users\Wan Amirul Asyraf\AppData\Local\Temp\WB_DESKTOP-4D6L530_Wan Amirul Asyraf_11836_2\unsaved_project_files\dp0\FFF\Fluent\fpac0.001.i
x-coord
y-coord
z-coord
pressure
x-velocity
```

FIGURE 4.2. The number of iterations to converge

## 4.2 Contour Distribution of water as the working fluid

Contour distribution is the graphical representation of the model after processing or solution unit. It can be obtained from post-processing or under result tab in Ansys Fluent. The function of investigating the contour distribution is to see the flow of the heat transfer in the model. Depending on the application, other than temperature and pressure, velocity also can be observed to study the motion. In this project, velocity will not be observed as it is not a critical parameter that should be obtained. Contour distribution investigation starts by observing the absorber plate as below:

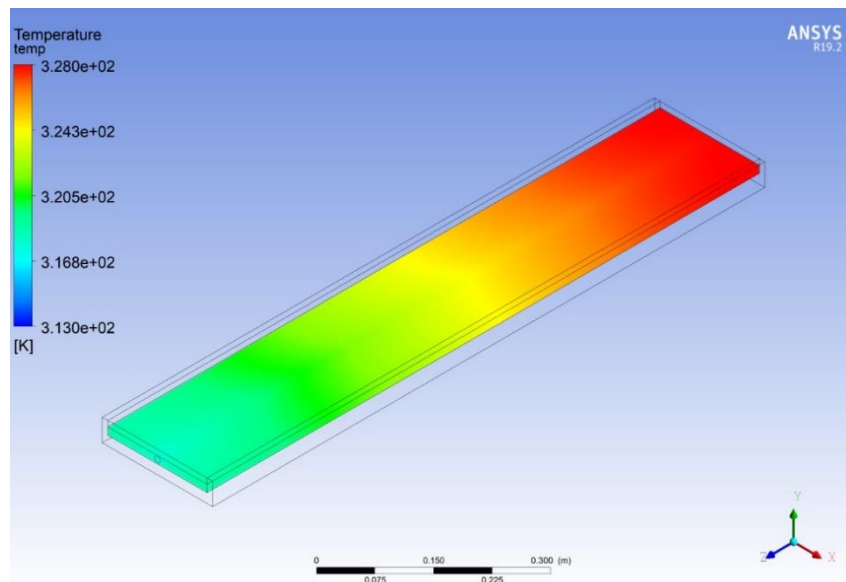


FIGURE 4.3. Temperature contour distribution of the absorber plate

As the main function of absorber plate is to receive the solar radiation and convert it into heat and transfer it to the working fluids. The contour distribution above represents its function at which the inlet part is colder comparing to the outlet part. As the fluids absorbing heat throughout the passage, heat transfer occurs hence increasing the temperature at the rear part of the flat plate solar collector.

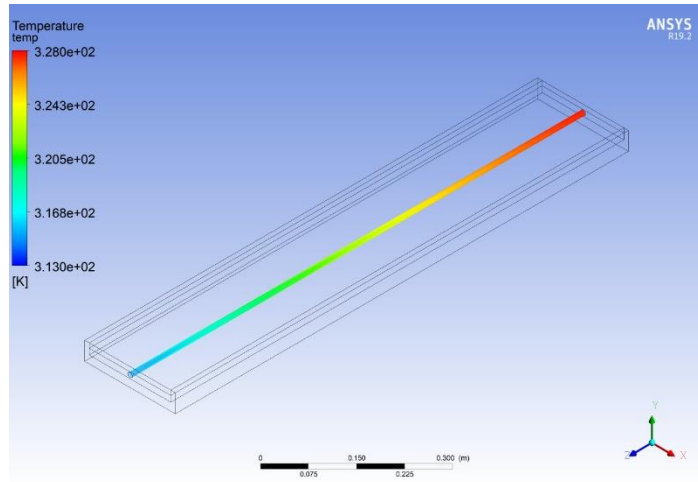


FIGURE 4.4. Temperature contour distribution of the fluid

Similar behaviour observed for the fluids section. It shows a uniform increment of the temperature across the collector length. The temperature visualisation range are set similar to the absorber plate contour and from the graphical representation above, the inlet fluid is a little bit colder compared to the front part of the absorber plate. This is due to the beginning of heat transfer starts to happen.

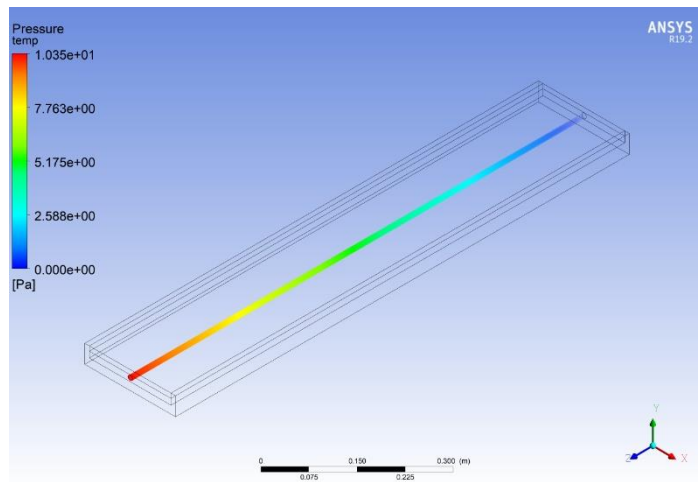


FIGURE 4.5. Pressure contour distribution of the fluid

It is expected to see pressure drop phenomenon in a fluid flow passage. The lowest pressure developed at the end of the tubes. The reason of pressure drop is due to the frictional forces acting on the fluid which introduced resistance to flow thought out the tube.

### 4.3 Code Validation

As there is no research paper uses vegetable oils as the working fluid in the flat plate solar collector, validation by using water will be used. Validation is important to make sure the model, geometry, boundary condition and cell zone condition are correct. Hence the data for validation progress will be retrieved from Ranjitha et al. (2013). They worked with both experimental and simulations works to validate their result with a very low percentage of error.

Few runs had been done by using water as the working fluid and the differences from the experimental results are being compared. Ranjitha et. al (2013) used mass flow rate of 0.025 kg/s for the inlet setup meanwhile in this project, velocity inlet of 0.02 m/s is used in the CFD software to match the setting as the geometry of is not exactly similar for simplicity purposes. Following is the relationship of the Ranjitha et. al (2013) experiment and the CFD result in this project:

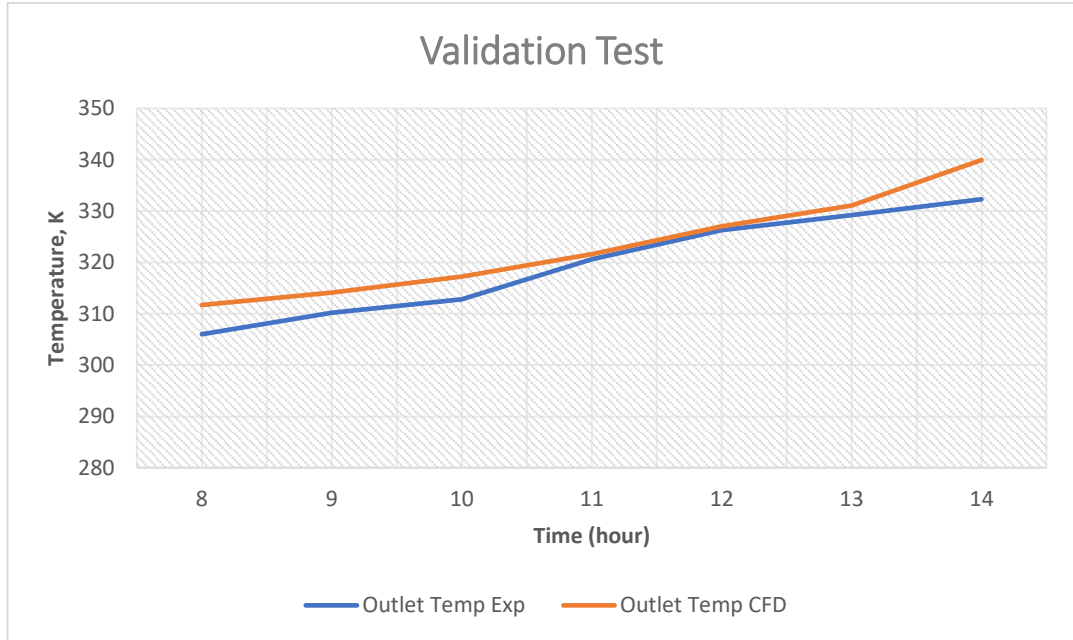


FIGURE 4.6. Validation Test Result

Seven runs had been tested in Ansys Fluent and the variable of the validation test are inlet temperature, time and radiation. Time and radiation are set under *Radiation* setting in Ansys Fluent according to the experimental data to match the working condition. All result from CFD are considered acceptable as the highest percentage different is at 2PM test which is 2.3%. The lowest is 12PM at 0.22% percentage different hence, this setting will be used to compare with vegetable oil.

#### 4.4 Vegetable oil based nanofluids efficiency vs nanoparticles concentration

CFD Simulations had been run for different number of concentrations with different type of nanofluids. Outlet temperature of each run will be observed to study the performance of the solar collector according to the governing equation of flat plate solar collector efficiency. The setting of each run follows the setup of 12PM study case such as the radiation value and the inlet temperature.

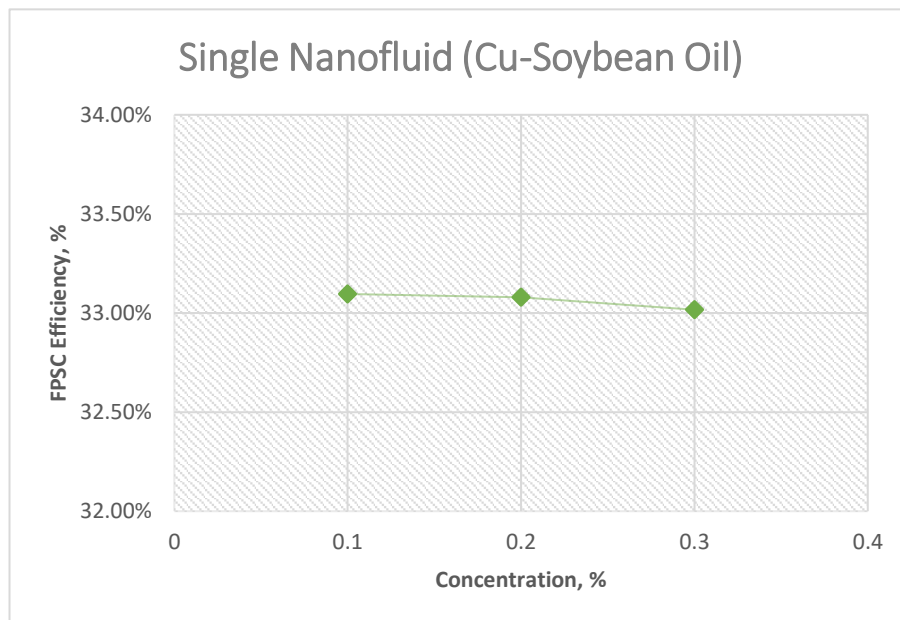


FIGURE 4.7. FPSC Efficiency vs Concentration % of Single Nanofluids (Cu-Soybean Oil)

From the obtained result, the performance of the solar collector nearly the same for all tested concentration. Even though it is expected that thermal conductivity is increased with the additional of nanoparticles onto the fluid, other thermal properties are sacrificed for example the dynamic viscosity and specific heat capacity. As concentration of nanoparticles are increased, dynamic viscosity is increased too which caused the outlet temperature to drop accordingly. For the specific heat capacity, it decreases with the percentage of concentration and it should significant drop for hybrid nanoparticles which drop at 0.3% concentration.

Based on single nanofluids graph, from 0.1% to 0.3% concentration, the efficiency shows a slight drop which cause a fluctuation pattern in graph. From this trend it can be concluded that as the concentration of copper nanoparticles in vegetable oil increase, efficiency of the solar collector will decrease as well. This might be because the viscosity increment is too high and this create the tendency of wall deposition phenomenon even though it show an increment in thermal conductivity.

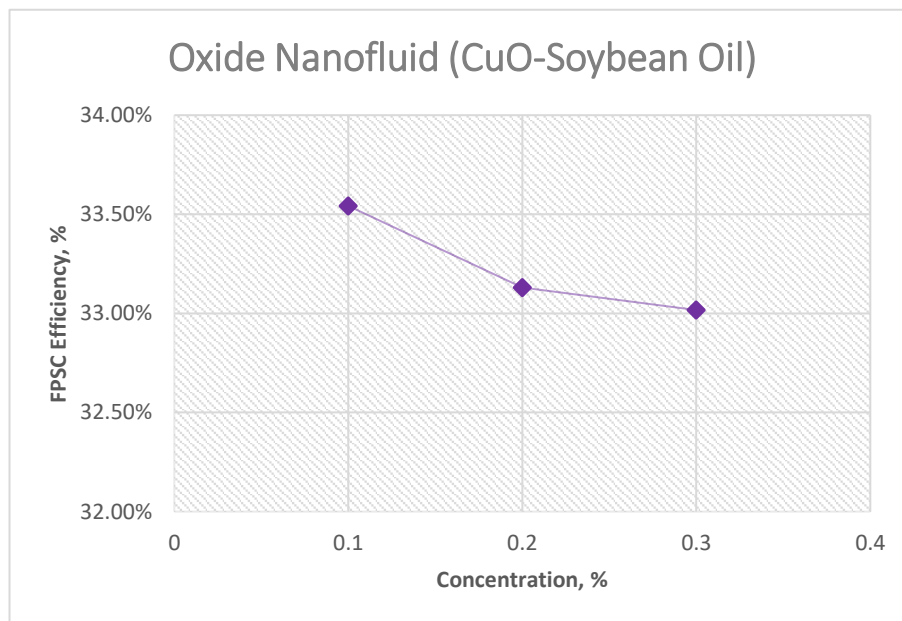


FIGURE 4.8. FPSC Efficiency vs Concentration % of Oxide Nanofluids (CuO-Soybean Oil)

For the oxide nanofluids on the other hand, shows almost similar pattern to the single nanofluids. However, the efficiency is much better at 0.1% concentration. This is because CuO nanoparticle has a better specific heat capacity under low concentration level. Besides, the density value is quite small compared to other nanofluid. The drop of efficiency from 0.1% to 0.2% is quite significant and it shows that under this range, the concentration of the nanoparticles shows a great effect on thermophysical properties of the nanofluids unlike the result from single nanofluid.

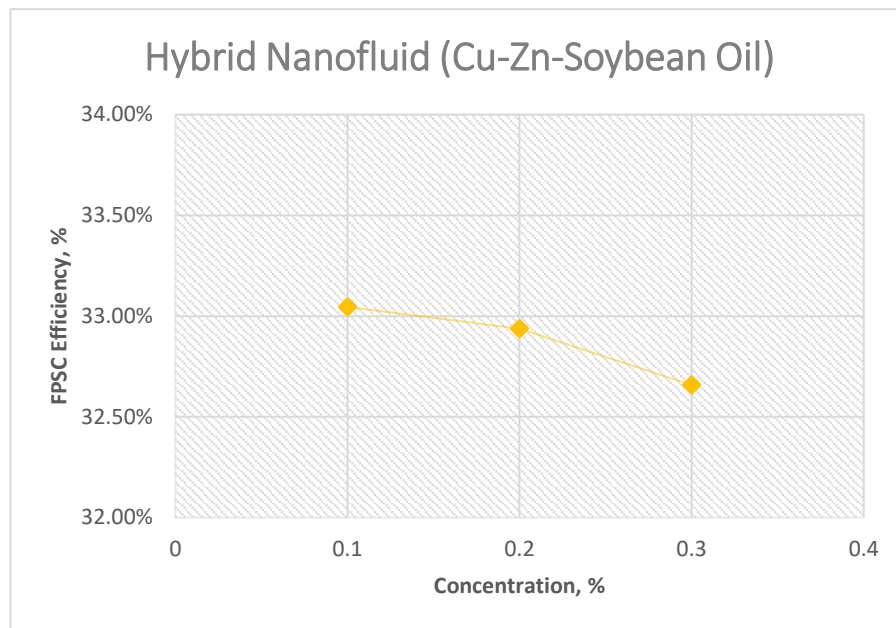


FIGURE 4.9. FPSC Efficiency vs Concentration % of Hybrid Nanofluids (Cu-Zn-Soybean Oil)

The trend shows the same pattern for hybrid nanofluids. However, the efficiency is significantly less under low concentration which is 33.05%. This shows that hybrid vegetable oil nanofluids is not suitable for fluid flow applications. Adding two different nanoparticles will cause a great thermal conductivity. However, the viscosity produced is quite big as well which will require more pumping power to resist the internal resistance in the fluid flow motion.

#### 4.5 Temperature Difference of different nanofluids

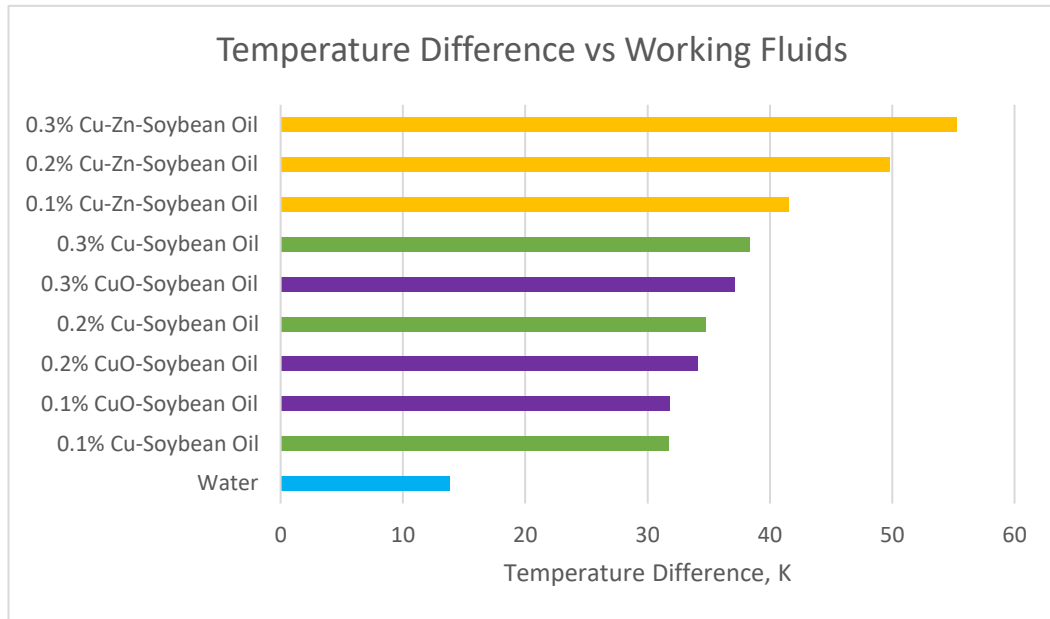


FIGURE 4.10. Temperature Difference for different working fluids

Inlet temperature are set to 313.2 K for all runs. Under same setting and conditions, temperature difference of all nanofluids are observed. This is crucial when the increment of temperature outlet is the prime factor for any application. According to the graph, the highest temperature difference at each concentration is hybrid nanofluid. Meanwhile for the pattern and trend, all three type of nanofluids exhibit the similar behavior in which, the temperature differences are slightly increase as the concentrations are increased. This is due to the decrement specific heat capacity value as nanoparticles are added in which small energy can be stored at each 1°C of a certain mass. This explains why water show a lower temperature difference comparing to the other nanofluids as the specific heat capacity is relatively large. However, the rate are different which hybrid nanofluids show the higher difference compared to single nanofluids and oxide nanofluids.



The reason why hybrid nanofluids achieve higher temperature difference is due to the the highest thermal conductivity enhancement at less viscous state compared to the other two fluids. Even though adding nanoparticles sacrifice a lot of specific heat capacity value compared to the other two fluids, hybrid nanofluid shows a thermal conductivity enhancement of 50% at 0.1% concentration meanwhile oxide and single nanofluid able to achieve approximately 30% at same concentration. Water on the other hand only able to achieve temperature different of 13.8 K. Hence, for the temperature increment, vegetable oil nanofluids surpass the conventional working fluid, water.

#### 4.6 Temperature Contour Distribution of Vegetable oils

From below temperature contour distribution, the red colour region at the outlet side is darker for the hybrid nanoparticles. Meanwhile, a slight dark for oxide nanofluids and lighter for single nanofluids. The objective to study the contour is observe the behavior of the nanofluids during irradiance energy from sun is being transferred on the solar collector. Following are the illustration based on the temperature contour of the tube:

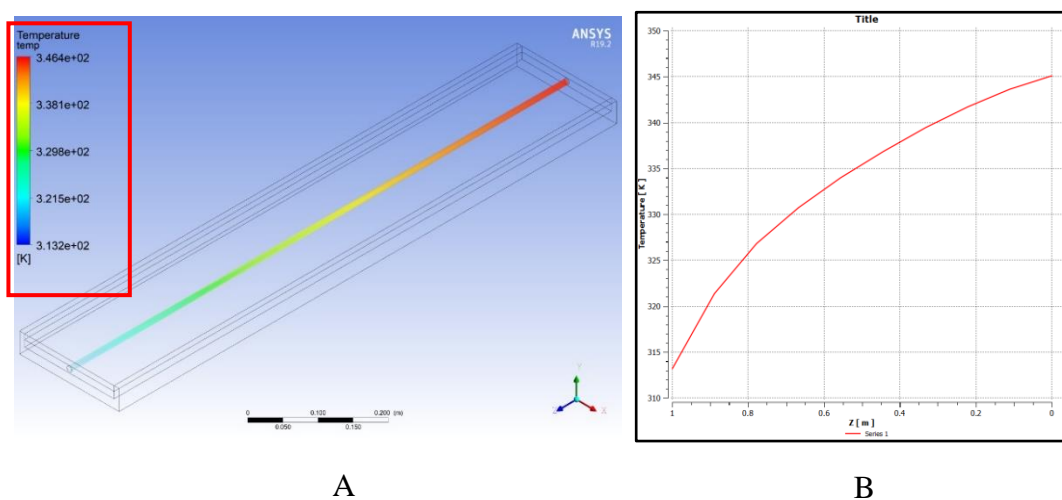


FIGURE 4.11. (A) Temperature distribution of single nanofluid at 0.1% concentration (B) Temperature vs length of the solar collector

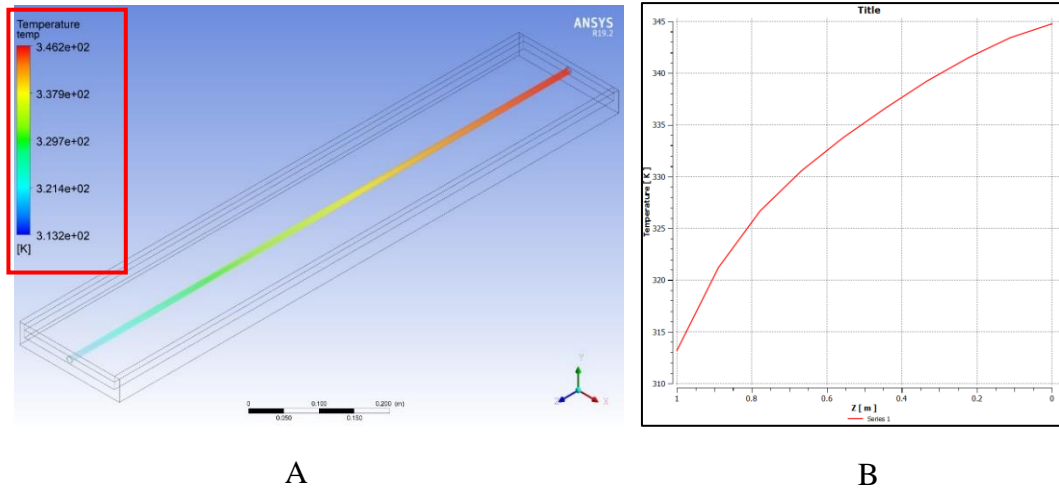


FIGURE 4.12. (A) Temperature distribution of oxide nanofluid at 0.1% concentration (B) Temperature vs length of the solar collector

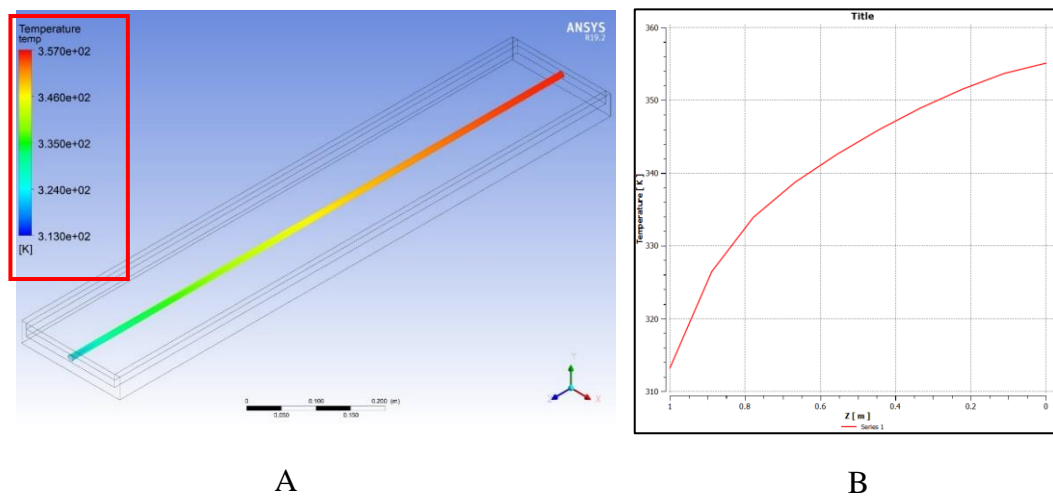


Figure 4.13. (A) Temperature distribution of hybrid nanofluid at 0.1% concentration (B) Temperature vs length of the solar collector

The box shows different temperature range even though the temperature contour is almost similar. The red contour at hybrid nanofluids indicates more higher temperature compare to single and oxide vegetables nanofluids. The show that show much hybrid nanofluids indicates faster heat transfer rate based on the contour in which the colour conversion from yellow to red appears earlier in the tube.

#### 4.7 Efficiency comparison among conventional fluids

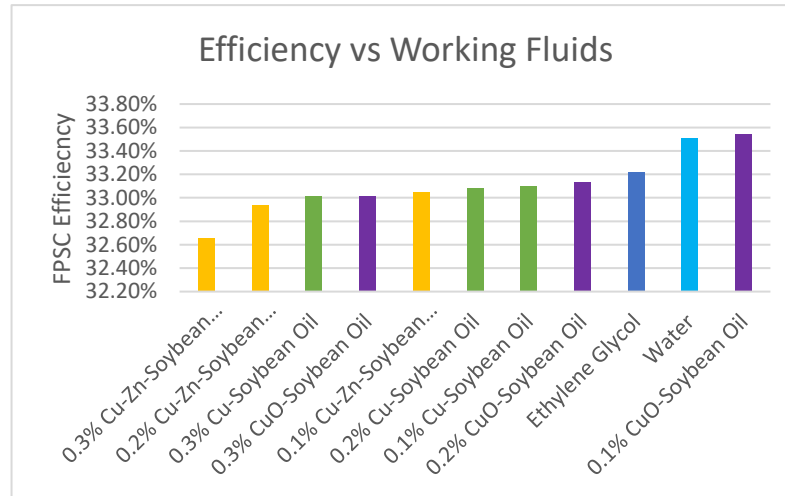


Figure 4.14. Working fluids efficiency comparison

At the end of this project, vegetable oils nanofluids are being compared with other conventional fluids such as water and ethylene glycol. According to the graph above, most of the vegetable oils has a lower efficiency compared to water. However, it does not mean it is not feasible to be used. The highest efficiency achieved is by using CuO-Soybean oil at 0.1% concentration which able to reach until 32.54% of flat plate solar collector efficiency. Meanwhile, water which dominates the result produces around 33.51%. This shows that nanoparticles greatly affect the flat plate solar collector efficiency and from this result, using CuO-Soybean oil at a very low concentration level will able to surpass conventional working fluid. By comparing with another conventional fluid which is ethylene glycol, the range of efficiency is almost in the same for both fluids. In this case, average vegetable oil nanofluid is a better option as ethylene glycol is well known with the toxicity and can harm the environment.

The best vegetable oil among the three nanofluids is 0.1% CuO-Soybean oil. This is because the efficiency is significantly different with the other nanofluids. One of the reasons is high enhancement under low concentration percentage. Under fluid flowing scenario, the viscosity matters the most and adding too much nanoparticles will eventually cause a disturbance for the flow and create wall deposition or internal resistance of the fluid to flow.

## 4.8 Discussion

As the performance study of vegetable oil as the working fluid in solar collector is totally depending on the formula to obtain the thermal properties value, the result might be less accurate as experimental data. This is because the formula obtained from classical models just like proposed by Maxwell or Einstein, is totally general and basic. Asadi et. al (2016) claimed that classical model formula generally underestimates thermal conductivity enhancement of nanofluids with nanoparticles loading. To get a very accurate data, formula should be created from experiment using the same vegetable oil based nanofluid as in this project.

Other than that, choosing the right nanoparticles is very important. From the result, different nanoparticles show a great influence and effect to the base fluid thermophysical properties. By using single and hybrid nanoparticles, the enhancement of efficiency could not be achieved and they behave differently under different concentration. For oxide vegetable nanofluids, efficiency improved even at a very small value. Meaning that, the tendency to enhance the performance further is high at a low concentration level.

The limitation of water is it freeze during winter. Draining the fluid may be one of the solutions however refueling back the system may not be perfect and air pocket can develop. Vegetable oil nanofluids as the alternative is introduced however it may need higher pump power is required. Comparing with water, vegetable oil may be recommended for an area that have winter season. This is because vegetable oil has lower freezing point compared to water.

From the obtained result, the relationship of solar collector efficiency and concentration of nanofluids can be observed. As we increase the concentration, the efficiency decrease even it increase the outlet temperature. This is because, the amount of temperature increment is not enough to improve the efficiency. Besides, the efficiency of all working fluid is less due to low mass flow rate input setting in CFD setting in order to match the pattern for the validation data trend. The efficiency can be improved further for all nanofluids when the mass flow rate increased.

## CHAPTER 5: CONCLUSION AND RECOMMENDATIONS

### 5.1 Conclusion

Numerical studies were conducted to study the performance of vegetable oil based nanofluids as the working fluids or the absorbing medium in flat plate solar collector. The conventional medium which is water shows a major drawback during winter season hence alternative for the fluid is proposed. Vegetable oil which is famous with interesting characteristic fluid such as environmentally friendly and free from sulphur compound which somehow may cause localized corrosion. To enhance the thermal properties of the vegetable oils, nanoparticles such as copper, copper (II) oxide and copper-zinc (hybrid) under different concentration are introduced to study the performance of the nanofluids in the solar collector. However, different nanoparticles will behave differently although the expectation on the thermophysical properties is better.

From this project, it is feasible to use vegetable oil as the working fluid with a little bit less efficiency. Due to less efficient performance, it is advised to use vegetable oil only in winter area as the major drawback of water is due to piping damage that result from freezing. Besides, in an area that lack a source of water also applicable to replace the conventional working fluid. For a better performance, it is suggested that the pumping power should be increased as oil is more viscous compared to water. Additional devices such as ultrasonic vibrator and mechanical stirring device are advised to be used as the stability of the nanofluids might be an issue especially in high temperature application that allow degradation rate to happen a lot faster. Chemical approach such as using Oleylamine as capping and reducing agent may be another solution to enhance the stability of oil based nanofluids.

## **5.2 Recommendations**

Closing the gap of accuracy is the majority goal in every research and project. As this project has in a limited timeframe, there are few suggestions for further analysis to obtain a perfect and accurate data for the performance study. Hence, I would like to recommend:

### **1) Experimental study**

This should be done with exact variable values or parameters so that numerical study and analysis can be compared apple to apple. Other than that, the benefit of having experimental work is the stability of the nanofluids and the exact behavior can be observed. Stability of nanofluids is very crucial to understand so that we can predict the lifespan before aggregation of nanoparticles occur over time. This can be done using photo capturing or DLS method.

### **2) Study the relationship between the efficiency vs Ti-Ta/G (reduced temperature value)**

The main function of studying this is to compare the nanofluids efficiency under specific operating range. For example, an application of increasing 30 C to 60 C is required and the best nanofluids may be different. To calculate the relationship, more time is required as the value of heat removal factor, F and overall heat loss coefficient should be determined, U<sub>I</sub> either from specification from factor or experimental data.

### **3) Adding stability device**

To consider using vegetable oil based nanofluids as the alternative to replace water, mechanical stirring device are recommended to be installed. Stability is one of the important factors especially when the nanofluids are subjected to high temperatures or repeating heating cycles as it affects the nanoparticles interplay and collision. Besides, other suggestion is the chemical approach by applying steric stabilization method that introduce the surface capping ligands.

## REFERENCES

- Aberoumand, S. & Jafarimoghaddam, A. (2017). Experimental study on synthesis, stability, thermal conductivity and viscosity of Cu–engine oil nanofluid. *J. Taiwan Inst. Chem. Eng.*, *71*, 315–322.
- Ahmadi, M. H., Mirlohi, A., Nazari M. A. & Ghasempour, R. (2018). A review of thermal conductivity of various nanofluids. *Journal of Molecular Liquids*, 181 – 188.
- Ahmed Kadhim, H. (2016). Applications of nanotechnology to improve the performance of solar collectors – Recent advances and overview. *Renewable and Sustainable Energy Reviews*, *62*, 767-792.
- Akoh, H., Tsukasaki, Y., Yatsuya, S. & Tasaki, A. (1978). Magnetic properties of ferromagnetic ultrafine particles prepared by vacuum evaporation on running oil substrate. *J Cryst Growth*, *45*, 495–500.
- Asadi, M., Rezaei, M., Siahmargoi, F. (2016). The effect of temperature and solid concentration on dynamic viscosity of MWCNT/MgO (20–80)–SAE50 hybrid nano-lubricant and proposing a new correlation: An experimental study. *Int. Commun. Heat Mass Transf*, *78*.
- Baek, M., Kim, M. K., Cho, H. J., Lee, J. A., Yu, J., Chung, H. E. & Choi, S. J. (2011). Factors influencing the cytotoxicity of zinc oxide nanoparticles: particle size and surface charge. *Journal of Physics: Conference Series*.
- Choi, S., Yu, W., Hull, JR., Zhang, ZG. & Lockwood, FE (2001). Nanofluids for vehicle thermal management. *Society of Automotive Engineers*, 139–144.
- Choi, S. In., Singer, D., Wang, H. (1995). Development and application of non-Newtonian flows. *New York: ASME*, *231*, 99-105.
- Dhinesh, K. D. & Valan, A. A. (2016). A review on preparation, characterization, properties and applications of nanofluids. *Renewable and Sustainable Energy Reviews*, *60*, 21-40.
- Edwin E., Garcia, R., Jane S.R.C. & Telis-Romero, J. (2013). Thermophysical Properties of Cotton, Canola, Sunflower and Soybean Oils as a Function of Temperature. *International Journal of Food Properties*, *16:7*, 1620 - 1629.
- Esfahani, N.N., Toghraie, D. & Afrand, M. (2018). A new correlation for predicting the thermal conductivity of ZnO–Ag (50%–50%)/water hybrid nanofluid: an experimental study. *Powder Technol*, *323*, 367–373.
- Fan, Y., Yingying, C., Liang, X., Jiale, Chiahsun, X., Lee, Q., Liang, P. & TaoTao, D. (2017). Dispersion stability of thermal nanofluid. *Progress in Natural Science. Materials International*, 531 – 542.

- Fasina, O. O. & Colley, Z. (2008). Viscosity and Specific Heat of Vegetable Oils as a Function of Temperature: 35°C to 180°C. *International Journal of Food Properties*, 11(4), 738-746
- Ghasemi, J., Jafarmadar, S. & Nazari, M. (2015). Effect of magnetic nanoparticles on the lightning impulse breakdown voltage of transformer oil. *Journal of Magnetism and Magnetic Material*, 4, 389.
- Hong, TK., Yang, HS. & Choi, CJ (2005). Study of the enhanced thermal conductivity of Fe nanofluids. *J Appl Phys*.
- Kai, S., Meyer, H., Gemel, C., Barthel, J., Roland, A & Janiak, C. Synthesis of Cu, Zn and Cu/Zn brass alloy nanoparticles from metal amidinate precursors in ionic liquids or propylene carbonate with relevance to methanol synthesis. *Nanoscale*.
- Kole, M. & Dey, T. K. (2013). Thermal performance of screen mesh wick heat pipes using water-based copper nanofluids. *Applied Thermal Engineering*, 50(1), 763–770.
- Maheshwary, P. B., Handa, C. C., & Nemade, K. R. (2017). A comprehensive study of effect of concentration, particle size and particle shape on thermal conductivity of titania/water based nanofluid. *Applied Thermal Engineering*, 79-88.
- Mahian, O., Kianifar, A., Sahin, A. Z., & Wongwises, S. (2014). Performance analysis of a minichannel-based solar collector using different nanofluids. *Energy Conversion and Management*, 88, 129-138.
- Maouassi, A. & Said, D. (2017). Numerical study of nanofluid heat transfer SiO<sub>2</sub> through a solar flat plate collector. *International Journal of Heat and Technology*, 35(3), pp. 619 – 625.
- Mukesh Kumar, P. C. & Muruganandam, M. (2017). A Review of Heat Transfer Enhancement Using Nano Fluids with Different Base Fluids. *Advances in Natural and Applied Sciences*, 8, 377 - 380.
- Muthukumar, T. Gnanaprakash, G. & Philip, Jo. (2012). Synthesis of Stable Magnetic Nanofluids of Different Particle Sizes. *Journal of Nanofluids*, 1, 85 - 92(8).
- Otanicat, T. (2010). Nanofluid-Based Direct Absorption Solar Collector. *Journal of Renewable and Sustainable Energy* 2, 033102.
- Rafiee, Z., Jafari, S.M., Alami, M. & Khomeiri, M. (2012). Antioxidant effect of microwave-assisted extracts of olive leaves on sun-flower oil. *J. Agric. Sci. Technol.* 14, 1497–1509.
- Ramasamy, D., Reddy, S., Ramachandran, T. & Gunasekharan, S. (2018). Experimental analysis of Thermal Performance of Solar Collector using CuO-H<sub>2</sub>O Nanofluid. *International Journal of Innovative Technology and Exploring Engineering (IJITEE)*, 8(2s2).
- Ranjitha, P., Somashekar, V., & Jamuna, A. B. (2013). Numerical Analysis of Solar Flat Plate Collector for Circular Pipe Configuration by using CFD. *International Journal of Engineering Research & Technology*. 2 (12).



- Saeeda, R. & Naza, S. (2019). Effect of heating on the oxidative stability of corn oil and soybean oil. *Grasas Y Aceites*, 70(2).
- Saeedinia, M., Akhavan-Behabadi, M.A & Razi, P. (2012). Thermal and rheological characteristics of CuO–Base oil nanofluid flow inside a circular tube.
- Saidur, R., Leong, K.Y. & Mohammad, H.A. (2013). A review on applications and challenges of nanofluids. *International Journal of Heat and Mass Transfer*, 57, 582–594.
- Sandeep, M.K., Vasu, V. & Gopal, A.V. (2016). Thermal conductivity and rheological studies for Cu–Zn hybrid nanofluids with various basefluids. *Journal of the Taiwan Institute of Chemical Engineers*, 66, 321–327.
- Sharif, M. Z., Rizalman, M., & Azmi., W. H. (2017). Improvement of nanofluid stability using 4-step UV-vis spectral absorbency analysis. Nano-Lubricant for Refrigeration. *Journal of Magnetism and Magnetic Materials* 389.
- Taylor, R. A., Patrick, E. P., Otanicar T. P., Chad, A. W., Monica, N., Trimble, S., & Prasher, R. (2011). Applicability of nanofluids in high flux solar collectors. *Journal of Renewable and Sustainable Energy*, 3.
- Tekir, M., Arslan, K. & Ekiciler, R. (2017). Numerical Simulation of Hybrid Nanofluid Flow in a Square Cross-Sectioned Horizontal Duct. *Conference Paper*.
- Vanek, F.M, and Albright, L.D., (2008). Energy Systems Engineering. *McGraw Hill*.
- Xuan, Y. & Li, Q. (2000). Heat transfer enhancement of nanofluids. *Int J Heat Fluid Flow*, 21, 58–64.
- Xuan, Y. & Roetzel, W. (2000) Conceptions for heat transfer correlation of nanofluids. *Int. J. Heat Mass Transf*, 43 (19), 3701–3707.
- Yua, F., Chena, Y., Liangb, X., Xua, J., Leea, C., Lianga, Q., Taa, P. & Denga. T (2017). Dispersion stability of thermal nanofluids. *Progress in Natural Science: Materials International*, 27, 531–542.
- Zhang, X., Gu, H. & Fujii, M (2006). Effective thermal conductivity and thermal diffusivity of nanofluids containing spherical and cylindrical nanoparticles. *J Appl Phys*, 100(4).
- Zhu, Q., Cui, Y., Mu, L. & Tang, L (2013). Characterization of thermal radiative properties of nanofluids for selective absorption of solar radiation. *Int J Thermophys*, 34(12).
- Zhu, H.T. & Yin, Y.S. (2004). A novel one-step chemical method preparation of copper nanofluids. *Journal of Colloid and Interface Science*, 227(1), 100-130.

## APPENDICES

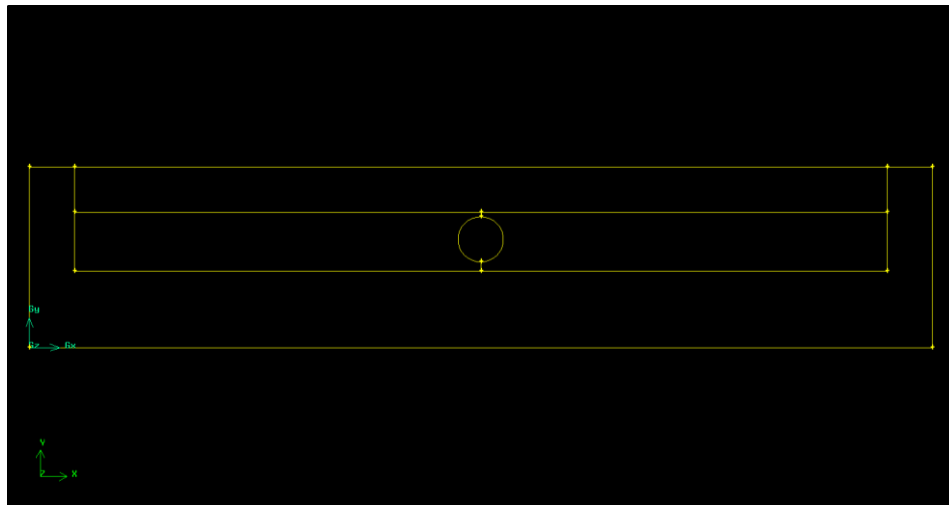


FIGURE A. 2D Drafting of the flat plate solar collector

```
Command> vertex create coordinates 0 0 0
Created vertex: vertex.1
Command> vertex create coordinates 0.2 0 0
Created vertex: vertex.2
Command> vertex create coordinates 0 0.04 0
Created vertex: vertex.3
Command> vertex create coordinates 0.01 0.04 0
Created vertex: vertex.4
Command> vertex create coordinates 0.19 0.04 0
Created vertex: vertex.5
Command> vertex create coordinates 0.2 0.04 0
Created vertex: vertex.6
Command> vertex create coordinates 0.01 0.03 0
Created vertex: vertex.7
Command> vertex create coordinates 0.1 0.03 0
Created vertex: vertex.8
Command> vertex create coordinates 0.19 0.03 0
Created vertex: vertex.9
Command> vertex create coordinates 0.01 0.017 0
Created vertex: vertex.10
Command> vertex create coordinates 0.1 0.017 0
Created vertex: vertex.11
Command> vertex create coordinates 0.19 0.017 0
Created vertex: vertex.12
Command> vertex create coordinates 0.1 0.024 0
Created vertex: vertex.13
Command> vertex create coordinates 0.1 0.029 0
Created vertex: vertex.14
Command> vertex create coordinates 0.1 0.019 0
Created vertex: vertex.15
Command> vertex create coordinates 0.105 0.024 0
Created vertex: vertex.16
Command> vertex create coordinates 0.95 0.024 0
Created vertex: vertex.17
Command> undo
Undone to: vertex create coordinates 0.95 0.024 0.
Command> vertex create coordinates 0.905 0.024 0
Created vertex: vertex.17
Command> undo
```

FIGURE B. Coordination commands in Ansys Gambit

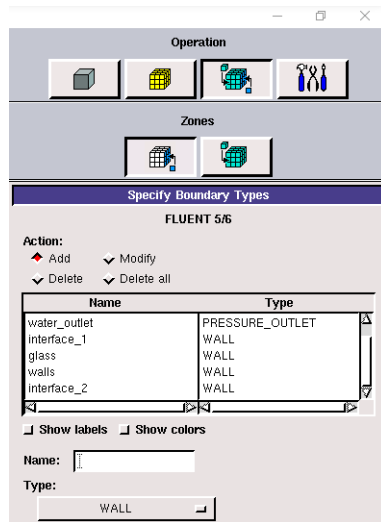


FIGURE C. Specifying boundary type in Ansys Gambit

**Nanofluids Thermophysical Calculator**  
by Wan Amirul Asyraf

| Base Fluids            | Soybean oil | Nano particles 1       | Cu   | Nano particles 2       |         |
|------------------------|-------------|------------------------|------|------------------------|---------|
| Thermal Conductivity   | 0.154       | Thermal Conductivity   | 18   | Thermal Conductivity   | 3332.99 |
| Density                | 913.7       | Density                | 6510 | Density                | 7100    |
| Specific Heat Capacity | 1957        | Specific Heat Capacity | 540  | Specific Heat Capacity | 390     |
| Dynamic Viscosity      | 0.028       | Concentration          | 0.3  | Concentration          | 0.15    |
| Concentration          | 0.45        |                        |      | Concentration of Hb    | 0.45    |

---

| Conventional Nanofluids | Hybrid Nanofluids |                        |             |       |
|-------------------------|-------------------|------------------------|-------------|-------|
| Thermal Conductivity    | 0.34494           | Thermal Conductivity   | 2.920025605 | W/mK  |
| Density                 | 2592.59           | Density                | 3520.535    | kg/m3 |
| Specific Heat Capacity  | 1531.9            | Specific Heat Capacity | 1082.63119  | J/kgK |
| Dynamic Viscosity       | 0.0683            | Dynamic Viscosity      | 0.124815011 | kg/ms |

FIGURE D. Example of program calculator with values

```

Calculation complete.

Area-Weighted Average
Total Temperature (k)
-----
liquid_inlet      313.28022
liquid_outlet     327.01312
-----
Net                320.14667
  
```

FIGURE E. Example of result retrieved from Ansys

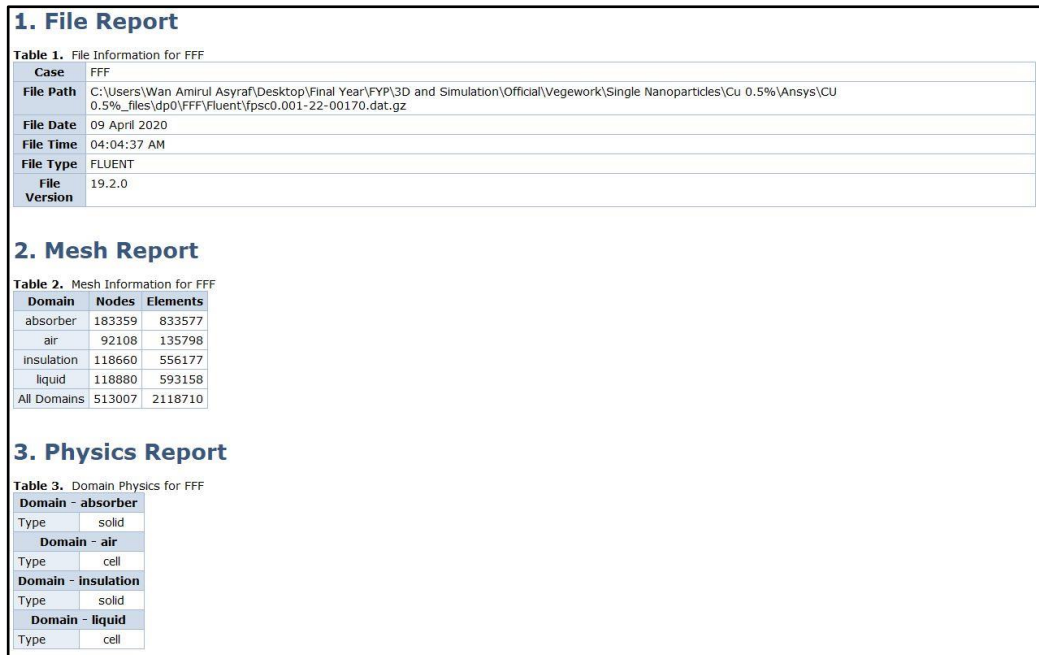


FIGURE F. File, Mesh and Physic Report from Ansys Fluent

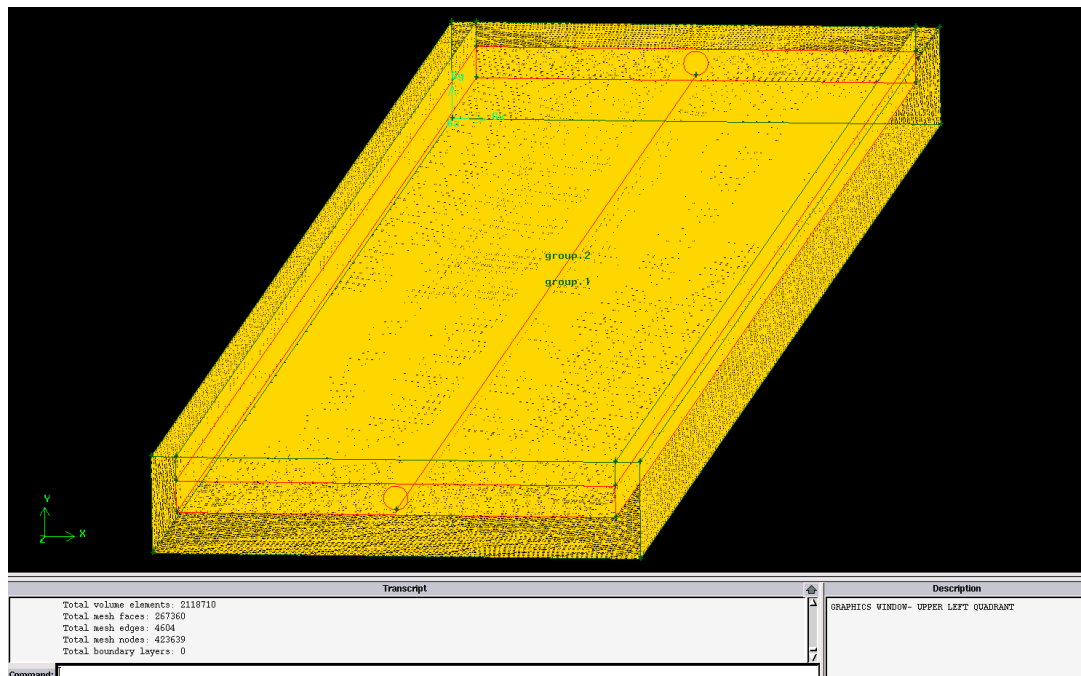


FIGURE G. Mesh transcript from Ansys GAMBIT